SYNTHESIS AND CHARACTERIZATION OF NEW (AROMATIC/HETEROCYCLIC-BASED) POLYMER SERIES FOR CARBON DIOXIDE CAPTURE

BY

Ahmed Mohamed Alloush

A Thesis Presented to the
DEANSHIP OF GRADUATE STUDIES

KING FAHD UNIVERSITY OF PETROLEUM & MINERALS

DHAHRAN, SAUDI ARABIA

In Partial Fulfillment of the
Requirements for the Degree of

MASTER OF SCIENCE

In

CHEMISTRY

May 2016

KING FAHD UNIVERSITY OF PETROLEUM & MINERALS

DHAHRAN- 31261, SAUDI ARABIA

DEANSHIP OF GRADUATE STUDIES

This thesis, written by **Ahmed Mohamed Alloush** under the direction his thesis advisor and approved by his thesis committee, has been presented and accepted by the Dean of Graduate Studies, in partial fulfillment of the requirements for the degree of **MASTER OF SCIENCE IN CHEMISTRY.**

Dr. Othman Charles Al Hamouz
(Advisor)

23/5/2016

Dr. Abdulaziz Al-Saadi

Department Chairman

M. A. Morsy

Dr. Mohamed Ali Morsy
(Member)

Dr. Salam A. Zummo
Dean of Graduate Studies

عمادة الدراسات العليا
DEANSHIP OF GRADUATE STUDIES

Dr. Bassem Al Maythalony
(Member)

26/5/16

Date

Dedication

To my beloved wife Toqa, dear parents, my brother & sister

& all my friends for their endless love & support

ACKNOWLEDGMENTS

All praise is to ALLAH Almighty who made it possible for me to accomplish this research work successfully.

First and the most important, I would like to thank my advisor Dr. Othman Al Hamouz for his guidance, support and patience during this research. His encouragement and insights enabled me to work towards getting desired results and to overcome the problems along the way. I would also like to thank all the amazing committee members Dr. Mohamed Morsy and Dr. Bassem Al Maythalony for their interest and valuable suggestions and support for this work by training and offering their lab facilities. I would also like to express my gratitude to all the faculty members of the Chemistry Department at KFUPM. To all of them, I appreciate what they have done to help me in my scholastic and professional growth.

I acknowledge my brother Rami for his amazing support and my dearest friends Sameh El Masry, Mahmoud Abdel Hakim, Abdullah Abo Elfadl and my research team members Mohamed Estaitie, Mahmoud Abd Elnaby & Adelabu Isaiah and all well-wishers, whom I have not mentioned above and whose best wishes have always encouraged me. Last but not the least I would like to thank my family who always supported me throughout my career and help in achieving my goals

TABLE OF CONTENTS

LIST OF TABLES

LIST OF FIGURES

LIST OF ABBREVIATIONS

AP1	:	Aniline-Pyrrole polymer (synthesized by Method 1)
$AP1_a$	:	Aniline-Pyrrole polymer (synthesized by Method 1) 1 Aniline: 2 Pyrrole molar ratio
$AP1_b$	:	Aniline-Pyrrole polymer (synthesized by Method 1) 1 Aniline: 1 Pyrrole molar ratio
AP2	:	Aniline-Pyrrole polymer (synthesized by Method 2)
AP3	:	Aniline-Pyrrole polymer (synthesized by Method 3)
AP4	:	Aniline-Pyrrole polymer (synthesized by Method 4)
P_o	:	Pyrrole polymer (synthesized by Method 1)
AF	:	Aniline-Furan polymer
AT	:	Aniline-Thiophene polymer
PFT	:	Pyrrole-Furan-Thiophene polymer
PFTA	:	Pyrrole-Furan-Thiophene-Aniline polymer

ABSTRACT

Full Name : Ahmed Mohamed Alloush

Thesis Title : SYNTHESIS AND CHARACTERIZATION OF NEW (AROMATIC/HETEROCYCLIC-BASED) POLYMER SERIES FOR CARBON DIOXIDE CAPTURING

Major Field : Chemistry

Date of Degree : May 2016

This work introduces the synthesis of a brand new polymers series consisting of five basic Polymers out of four monomers and one linker (Aniline, Pyrrole, Furan and Thiophene with Paraformaldehyde as the linker), using polycondensation reaction. The synthesis was carried out under different conditions for one polymer for the optimization to achieve the desired characteristics for carbon dioxide capturing application. These synthetic pathways used in the preparations produced polymers of different surface areas, pore characteristics, different yields, and slight change in the connectivity. Then polymers were triturated and activated. These polymers were then characterized by ^{13}C-NMR, FTIR, XPS and CHN elemental Analyzer for structure elucidation, powder XRD was used for determination of amorphousity and crystallinity level of the materials. Thermal properties were investigated using TGA and DSC. Then surface area, pore size analysis and SEM imaging for full identification of the surface properties, and then carbon dioxide sorption test. Furthermore, they were tested for selectivity toward carbon dioxide compare to nitrogen and methane gases adsorption as they have high contribution in the composition of the flue gas. Finally, the outcome of the work is evaluated by a comparison against any reference materials or other published work to identify the efficiency of the synthesized polymers in this study.

ملخص الرسالة

الاسم الكامل: أحمـد محمـد علـوش

عنوان الرسالة: تحضير وتوصيف مجموعة بوليمرات جديدة من وحدات أروماتية تستخدم في معالجة غاز ثاني أكسيد الكربون

التخصص: كيميــاء

تاريخ الدرجة العلمية: مايــو 2016

هذا العمل يعرض تحضير مجموعة بوليمرات جديدة مكونة من خمس بوليمرات مختلفة تم تحضيرها من أربع وحدات بنائية أساسية بالإضافة إلى المادة المستخدمة للربط بين الوحدات وهذه المواد هي (أنيلين, فيوران, ثيوفين, بيرول وفورمالديهيد) وتم تحضير هذه البوليمرات باستخدام ظروف تفاعل مختلفة في محاولة للوصول لأفضل مواصفات لاستخدام المادة في التطبيق المصنوعة له. استخدام هذه الظروف المختلفة أدى إلى الحصول على صفات مختلفة للمواد كمساحة السطح وطبيعة المسام وحجمها والذي أثر على قدرة المواد على امتصاص غاز ثاني أكسيد الكربون. بعد اختيار الطرق المناسبة للتحضير وتحضير المواد تم توصيف هذه المواد بطرق مختلفة لتوضيح طبيعة وكيفية ارتباط الوحدات المكونة لهذه البوليمرات بعضها ببعض حيث تم استخدام جهاز الرنين المغناطيسي النووي والأشعة تحت الحمراء وتحليل العناصر الأساسية. وتم أيضاً دراسة الصفات الحرارية للبوليمرات عن طريق جهاز التحليل الوزني الحراري. بعد الانتهاء من توصيف المواد بالأجهزة المذكورة وغيرها تم اختبار قدرة المواد على امتصاص غاز ثاني أكسيد الكربون بالإضافة إلى غازات أخرى وهي الميثان والنيتروجين لقياس قدرة المادة على الاختيار, وفي النهاية تم مقارنة النتائج مع مواد أخرى تم نشرها في أعمال بحثية مختلفة لتقييم قدرة المواد التي تم تحضيرها في هذا العمل.

CHAPTER 1

INTRODUCTION

In this study, a series of polymers, which is tested for sorption of CO_2 gas, were prepared. The sorption ability was examined at low pressures and different temperatures, to plot the isotherms, which is very important to estimate their efficiency for sorption. These polymers are not only prepared to be with high sorption capacity for CO_2, but also to have a selective property of CO_2 over N_2 gas and CH_4 gas, to make an estimation about the selective capturing property of CO_2 in flue gas, that facilitate and enhance the CO_2 sorption in mixture of gases, these properties are very important because the proper separation and sorption of CO_2 is a fundamental step in the CO_2 capture and sequestration (CCS) process.

The polymers are synthesized using two different approaches that are expected to make some differences in connectivity, networking, yield and degree of polymerization. After the synthesis of all polymers, they will be treated and optimized to be characterized and then tested for the capturing of CO_2 gas. Testing the polymers is a multistep procedure in which various physical, chemical and morphological properties were taken in consideration and investigated in details in order to provide the best illustration possible. So after synthesis and treatment, synthesized materials were triturated, activated and dried and became ready for characterization. Different instruments were used to determine the structure of the synthesized materials and their thermal properties. A detailed study was first done on one polymer (Aniline-Pyrrole), starting from different synthetic methods to

full characterization to a complete application and calculations, all of that was done prior to the involvement in the rest of the other polymers.

Testing the materials for CO_2 capturing was accomplished through several stages in order to determine the surface area of the materials, the pore size and pore distribution. And then the isotherms were measured at different temperatures, not only with CO_2 but with N_2 and CH_4 also. From the isotherms a lot of information were extracted mainly the predominant pore type to define the material as microporous, mesoporous, macroporous or even it may be a non-porous material. The pore type and isosteric heat of adsorption and of course the uptake capacity of the materials and their selectivities were also calculated and compared to each other and compared to other materials.

1.1 LITERATURE REVIEW

Witnessing the global climate change through all these years that is induced by greenhouse gases, especially the rapidly increasing concentration of CO_2 gas, in the atmosphere has stimulated active research fields to develop new and highly efficient techniques to be able to lessen CO_2 emission. This environmental problem that has become a major concern all over the globe [1], is directly related to a vast variety of industrial productions, Since CO_2 stems mainly form the combustion of the fossil fuel, which is an indispensable source given the continuous and increasing energy demand.

The synthesis of polymeric molecules with the property of carbon dioxide (CO_2) capturing, reflects the need of certain characteristics as high surface area, high degree of crosslinking, thermal stability and selectivity to CO_2 gas over other gases and the sorption

capacity and the ability to desorb, which is a very important property in order for these polymers to be reusable.

A lot of efforts were exerted in the process of synthesizing different materials that can be used in this applications or, of course, in other application as well. A wide range of materials were successfully synthesized as Zeolites [2], Porous Organic Polymers (POPs) [3], Metal Organic Framework (MOFs) [4] and Porous Silica with functional groups modification [5]. And since this work discusses polyamine polymeric materials, the main focus will be on Porous Organic Polymers.

Yao-Qi et al [6], in 2014, succeeded to fabricate new polymeric network out of two simple monomers, 2,4,6-tris(chloromethyl)mestylene and ethylenediamine, through the direct and simple nucleophilic substitution reaction under mild conditions in a catalyst free reaction. The reaction was carried out in three different solvents, tetrahydrofuran, 1,4-dioxane and ethyl acetate and the produced polymers were denoted as P1, P2 and P3 respectively. The resulted materials were found to be of high efficiency for CO_2 capturing and high selectivity over both N_2 and CH_4 gases, and as recorded in their work P2 and P3 reached uptake capacity of 57.6 and 56.2 mg/g respectively for CO_2 at 273K and 1.0 bar, while P1 scored the highest capacity under same conditions with 82.1 mg/g which is comparable to some high capacity reported adsorbents.

More recently in 2015, Pezhman et al [7], synthesized a novel porous polymer through a reaction between 2,6-pyridinedicarboxaldehyde and 1,3,5-tris(4-aminophenyl)benzene. The resulted polymer was then functionalized with Copper (II) tetrafluoroborate in order to increase its uptake capacity. The polymer had a BET surface area of 1580 m^2/g and enhancement of 200% in CO_2 uptake capacity at 0.15 bar and 273K

with 2.57 mmol/g uptake at 1.0 bar at same temperature, and 19% increase in the binding affinity.

Doyun Lee et al (2015) [8], managed to synthesize a porous polymer in a two-step process, first copolymerize divinylbenzene with 4-vinylbenzylchloride using radical polymerization, then the resulted polymer is surface modified with polyamines. The polymer without the polyamine treatment recorded 0.72 mmol/g CO_2 uptake at 1.0 bar and 273K, polyamine surface modification by ethylenediamine, diethylenetriamine, triethlenetetramine and tetraethylenepentamine resulted in significant higher uptake capacity of 1.49, 1.86, 1.86 and 1.82 mmol/g respectively at 1.0 bar and 273K.

The reason why all of these synthesized materials and others are good CO_2 hunters is back to the special characteristics of CO_2 gas such as the large quadrupole moment of CO_2 molecule (2.85) and its polarizability with taking in consideration the presence of the electron-deficient carbon atom are very important characteristics that distinguish this gas over others and can be used to design new CO_2-philic solids that do not only absorb it but also provide high selectivity, because depending on these facts CO_2 is believed to interact with protic electronegative functional groups like amines or azo groups [9], this approach has already been proven to be totally successful in enhancing the isosteric enthalpy of CO_2 adsorption especially with oxygen containing functional groups [10] and so, the presence of amino groups within these molecules is very important and develops significant absorptivity and selectivity, the most dominating method for capturing CO_2 is by applying flue gas or post-combustion gas through aqueous monoethanol amine (MEA) [11], since amines are known for their ability to bind with CO_2 via the formation of carbamate functional group [12][13].

The reaction that is used for this synthesis is a condensation polymerization process of Aniline and Paraformaldehyde in different temperatures and acidic conditions using hydrochloric acid in one synthesis [14] and Ferric chloride in the other [15] with active hydrogen compounds (Pyrrole – Furan – Thiophene).

The molecular structure of Aniline–formaldehyde copolymers was reported to depend on the molar ratios of aniline to formaldehyde in the polymerization process, to be either linear or cross-linked condensation polymerization process [16][17]. When aniline is in excess of formaldehyde in the polymerization solution, e.g., at the Aniline/Formaldehyde ratio of 1:0.5, a linear copolymer is probably formed, in which the amino group of aniline unit predominately exists as primary and/or secondary amines, and formaldehyde is added to the ortho- and/or para- positions of aniline during the condensation polymerization, By further increasing of formaldehyde concentration in the polymerization solution, the character of cross-linking copolymers with more benzoquinone units and less primary/secondary amine units were predominating [18].

Aniline formaldehyde condensate was reported with coated silica gel for metal removal application specifically, removal of hexavalent chromium [14]. The synthesis of this condensate was done in acidic conditions using concentrated hydrochloric acid at high temperature up to 100^{o}C, this procedure is reported for Liu and Freund [19] as they managed to synthesize a crosslinked polyaniline polymer via two step reaction, and the mentioned procedure was used as the first step to form the aniline formaldehyde condensate then the product was crosslinked with new aniline monomers via the free amine groups.

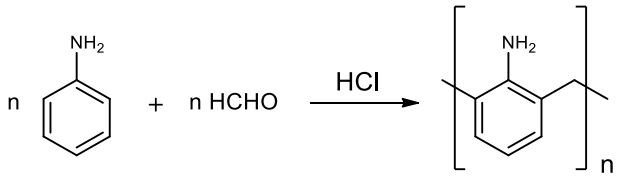

The copolymerization between the Aniline and Pyrrole, Furan or Thiophene using the methylene linkage from the paraformaldehyde, was not found in literature. But the homopolymerization of Aniline and of the heterocyclic rings was extensively studied in order to produce hyper-conjugated conductive polymers and recently were used in the production of supercapacitor electrode via the oxidative polymerization of the pyrrole on the surface MoS_2 producing nanocomposites of MoS_2 and ultrathin films or nanosheets of polypyrrole deposited on it [20].

Copolymerization of these heterocyclic rings was reported for pyrrole with N-substituted pyrroles, without any linkers again for maintain the property of conductivity. This work was by Yamamoto et al. in 2012 [21] and this copolymerization gave them higher thermal stability and higher conductivity compared to the homopolymerized unsubstituted pyrrole.

One of the main objectives of our work is to incorporate different functionalities in one material, it is a very important trend to go with and there is very recent work published on this topic in 2015 [22], the work shows a fertile functionalization of covalent organic polymers with up to five different functionalities in one material and after studying the effect of these functionalities on the properties of the material it was found that high porosity and remarkable hydrothermal stability along with high uptake of CO_2 gas was achieved.

There is a lot of work on hyper-crosslinked porous organic polymers, also known as (POPs) going on up to now because of the unlimited possibilities and the freedom in choosing the synthetic method that widen the field more and more. And since we are relating our work to POPs some unique works in this field will be discussed.

Yao et al. [23] in 2014 synthesized a hyper-crosslinked series of materials the exhibit a high BET (Brunauer–Emmet–Teller) surface area that goes up to 1980 m^2/g and uptake of 3.6 mmol/g at 273K and 1 bar. The material is comprised mainly of tetraphenylethylene connected by a methylene linkage arising from a formaldehyde dimethyl acetal compound using a Friedel-Drafts alkylation mechanism via the anhydrous iron(III) chloride.

In 2015, Liu et al. [24] worked on the synthesis of a series of polymers containing monomers of different number of benzene rings, the polymers were linked by a 1,3,5-tris(bromomethyl)-2,4,6-trimethylbenzene via a Friedle-Crafts alkylation reaction. The polymers were characterized as microporous materials and had a high surface area, depending on the surface area and pore type only the materials achieved high CO_2 uptake but because of the lack of any functional groups, the material was not remarkably selective for CO_2 and showed uptake for other gases also, beside that the isosteric heat of adsorption for the series was not very high and ranged in the region of the 20s kJ/mol which is consistent with the nature of the materials.

CHAPTER 2

ANILINE-PYRROLE POLYMER

2.1 Synthesis

All the polymers were synthesized after extensive modification and adjustment of the conditions in order to examine the effect of different solvent and different catalysts and their ratios along with the ratios of the monomers themselves aiming to achieve the best properties whether a higher thermal stability, better porosity, higher surface area, increase in the gas uptake or selectivity, etc. All these modifications were studied on the Aniline-Pyrrole (AP) copolymer.

A polycondensation reaction was used in the polymerization of Aniline, Pyrrole, Furan, Thiophene and p-formaldehyde using Two different synthetic routes that differ in the catalyst. In each synthetic method further modifications were applied, but here we are just proposing a mechanistic pathway that may represent the major route in the synthesis of these copolymers.

- **First synthetic route**, Hydrochloric acid will be used as the catalyst and DMSO will be the solvent and the reactions will be operated under 90^{o}C for 24 hours. The proposed mechanism for this reaction is illustrated in the following figure, (**Figure 1**).
- **Second synthetic route**, Ferric chloride will be the catalyst in DMSO and reactions will be operated under 80^{o}C for 24 hours. Possible proposed mechanism is shown in (**Figure 2**).

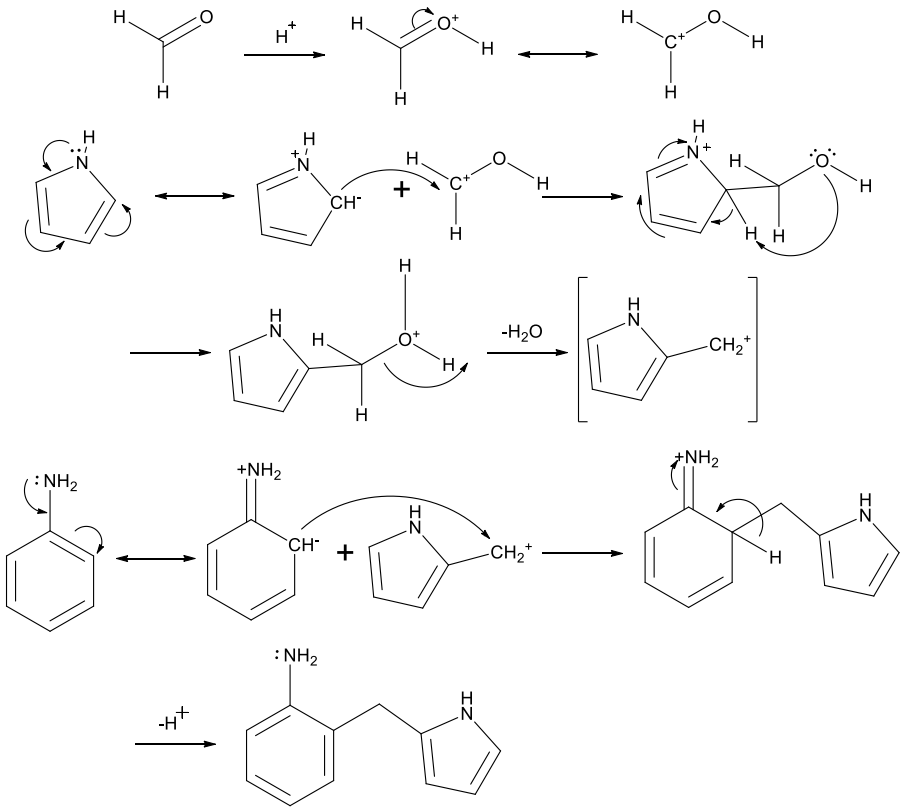

Figure 1 General proposed polycondensation mechanism for the series, where X can be N, O or S

These mechanisms were not proposed depending on kinetic study, and there is no proof whether the reaction goes via S_N1 or S_N2 mechanism but the free carbocation was introduced here as a transition state because generally bulky material are less likely to undergo bimolecular reaction. So, these mechanisms were proposed to clarify the general attack mode and the sequence in which this polycondensation reaction takes place, and to show the general proposed connections for the synthesized polymers.

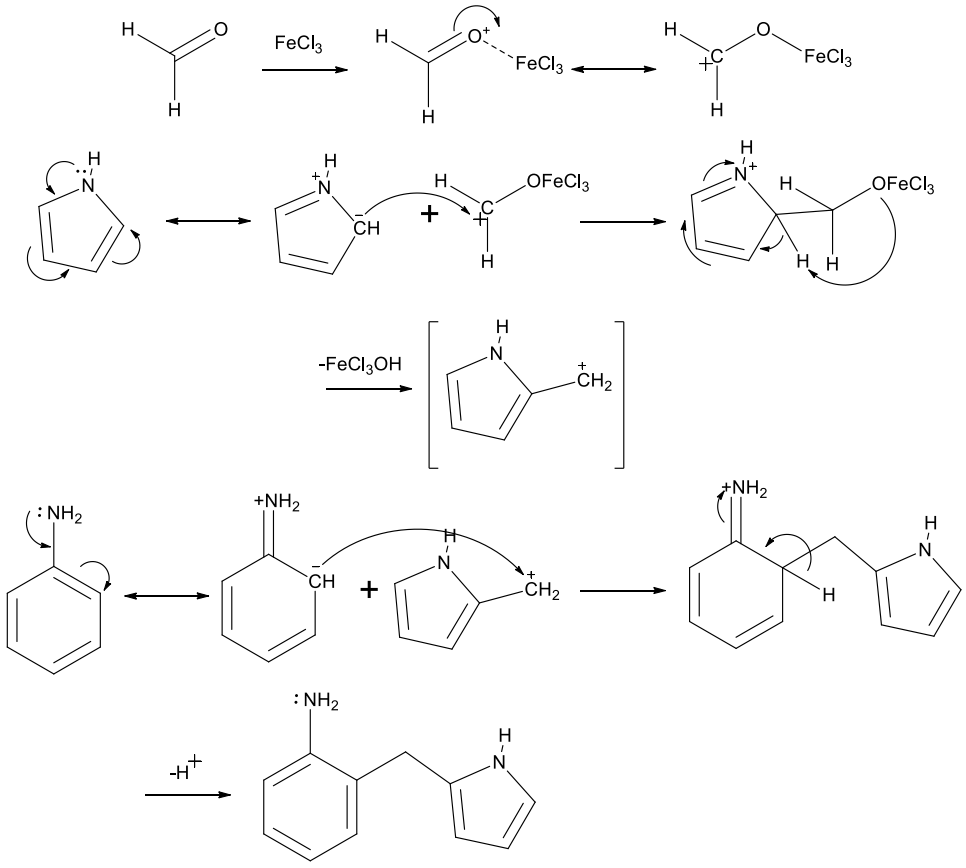

Figure 2 General proposed polycondensation mechanism for the series, where X can be N, O or S

2.1.1 Experimental details on the Aniline-Pyrrole (AP) polymer

Different methods and conditions were used in the synthesis of the Aniline and pyrrole co-polymer (AP) differing in the catalyst used and the temperature applied to reaction vessel and the solvent and also the molar ratios of the monomers, with almost constant time for the reaction. The general scheme of the Aniline-Pyrrole polymerization reaction made at different conditions is shown in (**Figure 3**), the molar ratios provided in this scheme are constants in the different procedures but was only changed for the investigation of molar ratios effect between Aniline and pyrrole in method (1) as will be explained in that section.

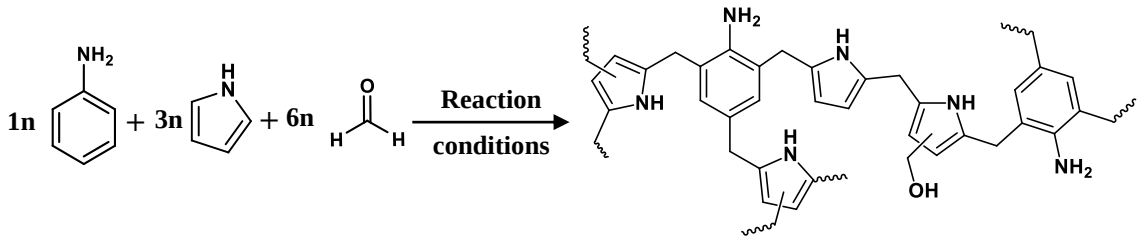

Figure 3 General reaction scheme for Aniline-Pyrrole polymer as synthesized under different conditions

Chemicals: Aniline (≥ 99.5%), Pyrrole (98%), Hydrochloric acid (HCl, 37%), Dimethylsulfoxide (DMSO, ≥ 99.9%) and Thionyl chloride ($SOCl_2$, ≥ 99%) were purchased from Sigma-Aldrich™ Co., Iron (III) chloride ($FeCl_3$) and Paraformaldehyde (H2O < 1%) were purchased from Fluka™ AG, N,N-dimethylformamide (DMF, 99%) from Alpha chemika™, Methanol (MeOH, ≥99.9%) and Ethanol (EtOH, ≥99.8%) were purchased from Merck Millipore™, and ammonium hydroxide solution (NH_4OH, 28-30%) from Fisher Scientific™.

2.1.1.1 Method (1) Reaction with Hydrochloric acid (HCl) catalyst at 90°C in DMSO solvent.

As pyrrole is sensitive to light and darkens upon exposure to air, it was distilled immediately before use and other chemicals were used as received without any extra treatment. The Linker p-formaldehyde (0.06 mol) was added first to reaction flask followed by (25 ml) DMSO, then the monomers Aniline (0.01 mol) with Pyrrole (0.03 mol) were added. The mixture is then stirred for few minutes and the catalyst (conc. HCl, 0.5 ml) was added while stirring, then introduced immediately to the oil-bath at 90^{o}C.

After the solid was obtained from reaction vessel, the solid is treated with different solvents in order to get rid of all unreacted material and to replace the solvent used in the

synthesis with a lighter solvent to obtain a pure solid as much as possible. The solid is then dried under vacuum for several hours (6-7 hrs.) at 70^{o}C. This same procedure exactly as described above was used to synthesize two other different AP copolymers that differ in molar ratio of the pyrrole species, one of them is **(AP1$_a$)** in which pyrrole was used as (0.02 mol), and the other is **(AP1$_b$)** with (0.01 mol) of pyrrole as described below:

Table 1 Experimental details for AP1, AP1$_a$ and AP1$_b$ polymers.

(AP1)				
Reaction Components				
Aniline (0.01 mol)	Pyrrole (0.03 mol)	Paraformaldehyde (0.06 mol)	DMSO	Conc. HCl (0.006 mol)
0.95 g	2.013 g	1.80 g	25 ml	0.5 ml
Temperature: 90°C		Time: 24 hours		Yield: 84%
(AP1$_a$)				
Reaction Components				
Aniline (0.01 mol)	Pyrrole (0.02 mol)	Paraformaldehyde (0.06 mol)	DMSO	Conc. HCl (0.006 mol)
0.93 g	1.36 g	1.81 g	25 ml	0.5 ml
Temperature: 90°C		Time: 24 hours		Yield: N/A
(AP1$_b$)				
Reaction Components				
Aniline (0.01 mol)	Pyrrole (0.01 mol)	Paraformaldehyde (0.06 mol)	DMSO	Conc. HCl (0.006 mol)
0.94 g	0.67 g	1.805 g	25 ml	0.5 ml
Temperature: 90°C		Time: 24 hours		Yield: N/A
Trituration: Methanol → Diethyl ether → Ammonia soln. → Distilled water → Methanol				

2.1.1.2 Method (2) Reaction with paraformaldehyde equivalence of Hydrochloric acid (HCl) at 150°C in DMF solvent.

This reaction was performed under kind of harsh conditions, from high temperature and high equivalence of acid. As pyrrole is sensitive to light and darkens upon exposure to air, it was distilled immediately before use and other chemicals were used as received without any extra treatment. The components were added in the following sequence, DMF (10 ml), Aniline (0.01 mol), pyrrole (0.03 mol) then the mixture was stirred for 2-3 minutes then the linker paraformaldehyde (0.06 mol) was added followed by the remaining solvent DMF (15 ml) and finally the hydrochloric acid (0.06 mol) was added with the mixture being stirred to achieve best possible homogeneity, then the reaction vessel was introduced to the oil-bath at 150ºC for 24 hours.

After the solid was obtained from reaction vessel, the solid is treated with different solvents in order to get rid of all unreacted material and to replace the solvent used in the synthesis with a lighter solvent to obtain a pure solid as much as possible. The solid is then dried under vacuum for several hours (6-7 hrs.) at 70°C.

Table 2 Experimental details for AP2 polymer.

(AP2)				
Reaction Components				
Aniline (0.01 mol)	Pyrrole (0.03 mol)	Paraformaldehyde (0.06 mol)	DMF	Conc. HCl (0.06 mol)
0.939 g	2.013 g	1.804 g	25 ml	5.0 ml
Temperature: 150°C		Time: 24 hours		Yield: 83%
Trituration: acetone → chloroform → ethanol → activation with methanol for 3 days				

2.1.1.3 Method (3) Reaction with Iron (III) Chloride ($FeCl_3$) catalyst at 80°C in DMF solvent.

This method differs from the first one in the catalyst, temperature & solvent. monomers' stoichiometric ratios are kept the same as Aniline (0.01 mol), Pyrrole (0.03 mol) and Paraformaldehyde (0.06 mol). As pyrrole is sensitive to light and darkens upon exposure to air, it was distilled immediately before use and other chemicals were used as received without any extra treatment. p-formaldehyde (0.06 mol) was added first followed by DMF (25 ml), then monomers were added and the mixture started stirring, then Iron (III) Chloride (0.004 mol) was added during the stirring at the end and the reaction vessel was added directly to the oil-bath at 80°C.

After the solid was obtained from reaction vessel, the solid is treated with different solvents in order to get rid of all unreacted material and to replace the solvent used in the synthesis with a lighter solvent to obtain a pure solid as much as possible. The solid is then dried under vacuum for several hours (6-7 hrs.) at 70°C. The elementary analysis for the product of this reaction was found, C, 73.4; H, 7.2; N, 14.3

Table 3 Experimental details for AP3 polymer.

(AP3)				
Reaction vessel components				
Aniline (0.01 mol)	Pyrrole (0.03 mol)	Paraformaldehyde (0.06 mol)	DMF	$FeCl_3$ (0.006 mol)
0.935 g	2.034 g	1.804 g	25 ml	0.96 g
Temperature: 80°C		Time: 24 hours		Yield: 86%
Trituration: Methanol → Diethyl ether → Ammonia soln. → Distilled water → Methanol				

2.1.1.4 Method (4) Reaction with Anhydrous Iron (III) Chloride ($FeCl_3$) Catalyst starting at Room Temperature (RT) and elevating gradually to (90°C) in DMF solvent & N_2 atmosphere.

For this reaction $FeCl_3$ was first treated to make sure it's anhydrous, (20 g) of the $FeCl_3$ were added to a round bottom flask and mixed with (50 ml) $SOCl_2$ and kept under reflux for 2 hours, then dried under vacuum and stored under nitrogen as iron-black powder with green iridescence. As pyrrole is sensitive to light and darkens upon exposure to air, it was distilled immediately before use and other chemicals were used as received without any extra treatment. This reaction was performed under nitrogen atmosphere, so except for the solids monomers and solvent were added after reaction flask was filled with nitrogen. First, paraformaldehyde (0.06 mol) and anhydrous $FeCl_3$ were added and flask was then sealed with a septum. After replacing the air in the flask with nitrogen, DMF (10 ml) was added followed by addition of Aniline (0.01 mol) and pyrrole (0.03 mol) simultaneously. Reaction starts and proceeds 6-7 hours at room temperature, then it is introduced to oil-bath adjusted at 50^{o}C until it completes 24 hours from the beginning of the reaction. Finally, the temperature was elevated to 90°C for about 4 hours.

After the solid was obtained from reaction vessel, the solid is treated with different solvents in order to get rid of all unreacted material and to replace the solvent used in the synthesis with a lighter solvent to obtain a pure solid as much as possible. The solid is then dried under vacuum for several hours (6-7 hrs.) at 70^{o}C.

Table 4 Experimental details for AP4 polymer.

(AP4)				
Reaction vessel components				
Aniline (0.01 mol)	Pyrrole (0.03 mol)	Paraformaldehyde (0.06 mol)	DMF	Anhydrous $FeCl_3$ (0.006 mol)
0.94 g	2.06 g	1.81 g	10 ml	0.97 g
Temperature: RT–50-80 °C		Time: 28 – 30 hours		Yield: 85%
Trituration: Methanol → Diethyl ether → Ammonia soln. → Distilled water → Methanol **(Sonication is used)**				

All the previously illustrated synthesis methods for AP polymer are briefly summarized in (**Table 5**) providing the reaction conditions and yields for each reaction.

Table 5 Main changes and differences in the preparation methods used in the synthesis of AP polymer

Polymer Name	**Catalyst**	**Solvent**	**Temperature[(a)]**	**Time**	**Yield[(b)]**
AP1	Conc. HCl	DMSO	90°C	24 hrs.	84%
AP2	Conc. HCl	DMF	150°C	24 hrs.	83%
AP3	$FeCl_3$	DMF	80°C	24 hrs.	86%
AP4	Anhyd. $FeCl_3$	DMF	R.T. - 50°C -90°C	28 – 30 hrs.	85%

(a) Temperature was kept constant in all the procedures except for (AP4) it was monitored as illustrated in the synthesis section.

(b) Yields are calculated after fully finishing the trituration process described in the synthesis section.

2.2 Characterization

Different characterization techniques were incorporated to investigate the nature of the synthesized polymer using the previously mentioned methods, these techniques are:

Nuclear Magnetic Resonance (NMR), Fourier-Transform Infrared (FT-IR), Thermal Gravimetric Analysis (TGA), Differential Scanning Calorimetry (DSC) and the surface area was also measured to choose the best synthesis method for the application but it will be illustrated in the section 2.3.

2.2.1 Solid state Nuclear Magnetic Resonance (^{13}C-NMR)

Natural abundance ^{13}C solid state NMR spectra were obtained on a **Bruker 400 Mhz** spectrometer operating at 125.65 MHz (11.74 T), at ambient temperature of 25^{o}C. Samples were packed into 4 mm zirconium oxide rotors. Cross polarization and high power decoupling were employed. Pulse delay of 5.0 s and a contact time of 2000.0 µs were used in the CPMAS experiments. The magic angle spinning rate was 10 kHz. ^{13}C chemical shifts were referenced to TMS by setting the high frequency isotropic peak of solid adamantine to 29.5 ppm.

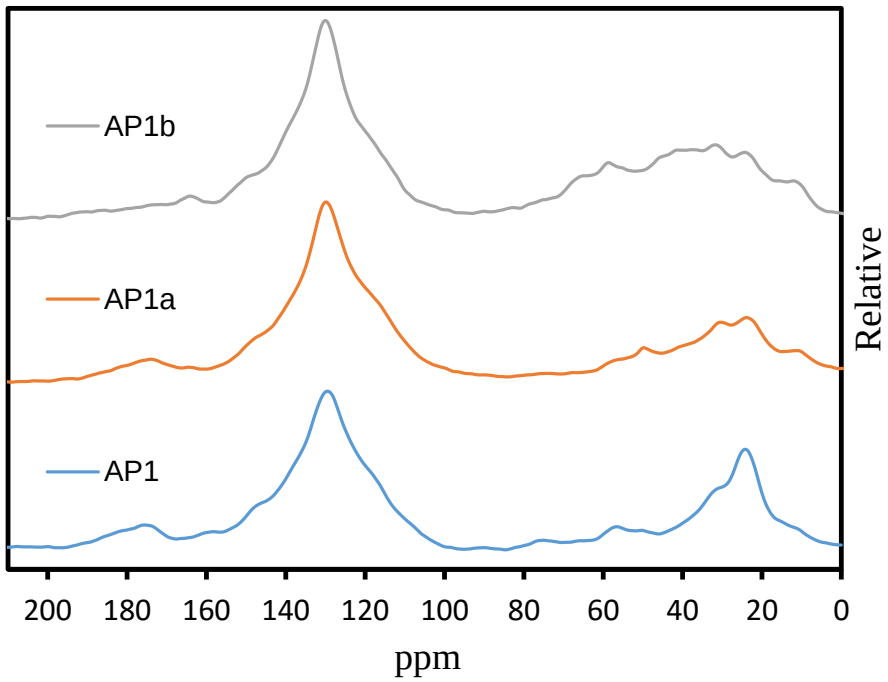

Figure 4 ^{13}C-NMR spectra of AP1 polymers of different molar ratios

From the comparison shown in (**Figure 4**), it is obvious that the percentage of Aniline monomer in the reaction under the same conditions, has its own effect on the peaks observed in the aliphatic region. It can be almost confirmed that all the peaks are observable in the three spectra but the intensities are different. Not all of these peaks can be defined with confidence, since the number of probabilities that this kind of polycondensation reaction is quite big.

In order to make this comparison more beneficial and to get rid of some doubts like the probability of the exclusion of Aniline from the reaction at lower percentages or the presence of the Aniline only between the pores of the polymers as if it is only trapped with no chemical or covalent connections, we had to perform another reaction that contains only Pyrrole and Paraformaldehyde. The reaction of Pyrrole and Paraformaldehyde (Pyrrole Only or P_0) was performed in the same conditions used for the synthesis of the three polymers AP1, $AP1_a$ and $AP1_b$. The ^{13}C-NMR spectrum for (P_0) is given in (**Figure 5**) and shows a different connectivity than what we have in the other three polymers containing the Aniline.

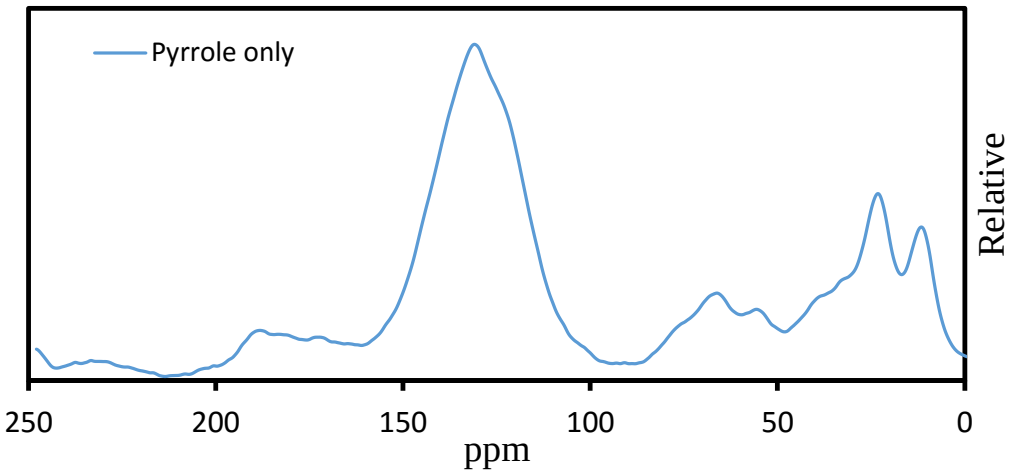

Figure 5 ^{13}C-NMR spectrum for Pyrrole Only (P_O)

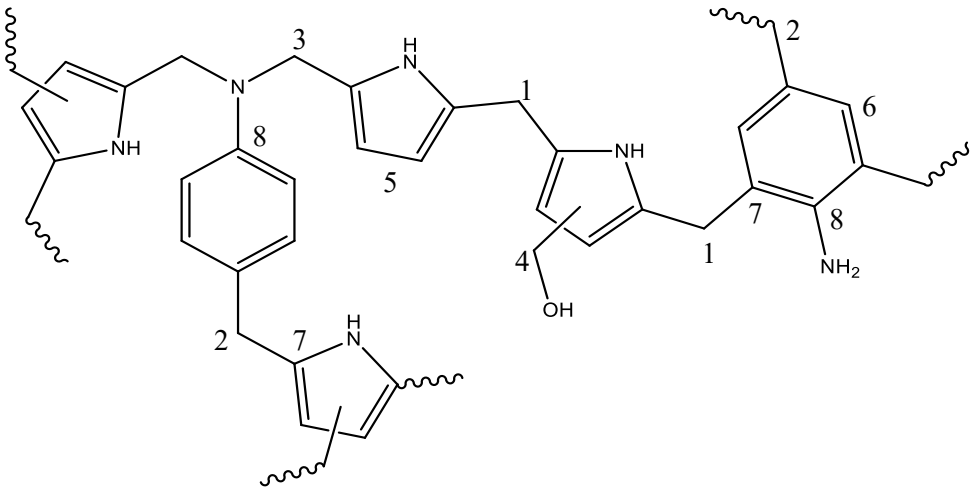

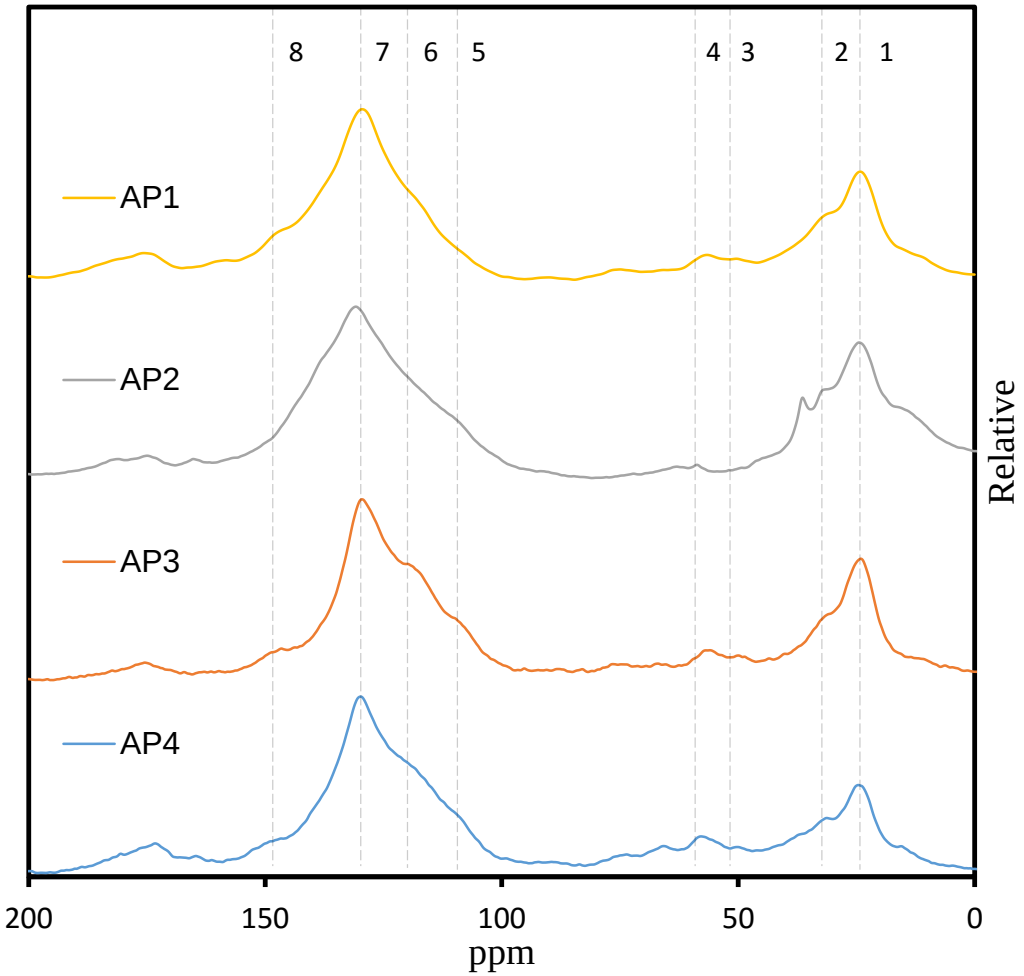

Figure 6 All ^{13}C-NMR spectra of (1:3) Pyrrole: Aniline AP polymers from different preparation methods

2.2.2 Fourier Transform Infrared Spectroscopy (FTIR)

The solid state Infrared spectra were investigated for the detection of functional groups All the data were obtained using a *Perkin Elmer 16F PC FTIR* spectrometer using solid potassium bromide (KBr) pillets in a region of 4000-400 cm^{-1} (mid-IR region).

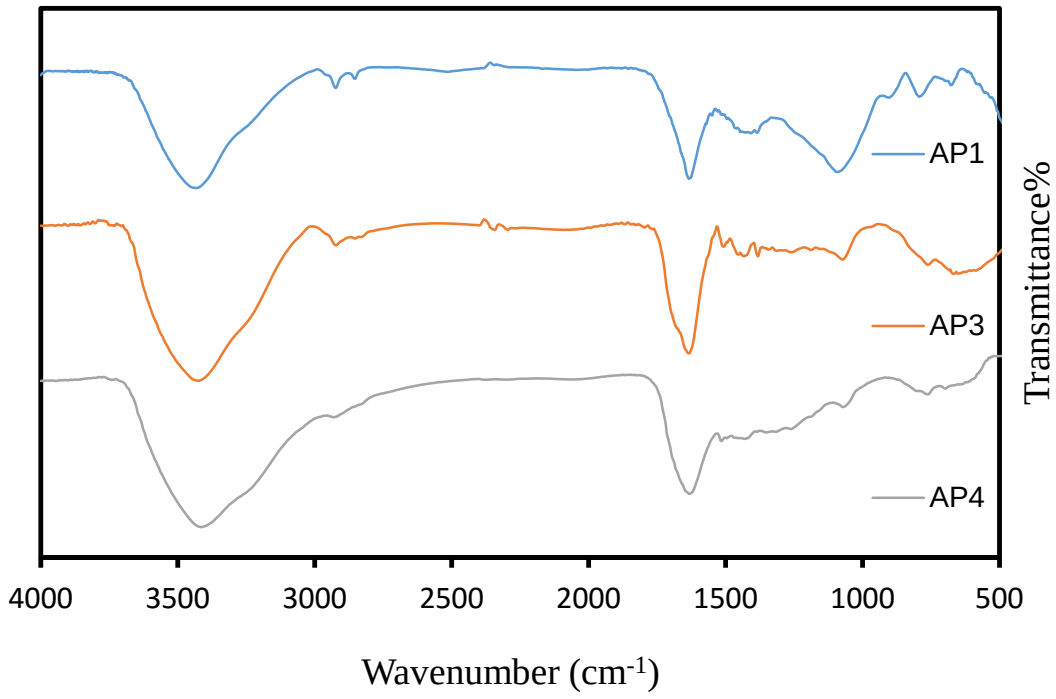

Figure 7 FT-IR spectra of AP polymers from different preparation methods

AP polymers in (**Figure 7**) show similar FT-IR spectra generally which was highly expected since same monomers were used and they can be considered as a one polymer at the end. For the characterization of the main bands, a broad band in the region from 3300-3500 cm^{-1} because of the overlap between the two peaks of 1° amine of Aniline and 2° amine pyrrole peak, besides there is a probability of the presence of hydroxyl (OH) group at the end of the chains as shown in the structural model made in (**Figure 6**) ,along with the NMR spectra, and at 1631 cm^{-1} the medium to strong NH_2 scissoring can be observed

overlapped with the C=C aromatic peaks that appears in the same region, NH_2 and NH wagging at 694 and 755 cm^{-1}.

2.2.3 Thermal Properties

2.2.3.1 Thermal Gravimetric Analysis (TGA)

Thermogravimetric analyzer that was used to conduct the analysis is *STA 429*® (NETZSCH group - Germany). The analysis was done under completely same conditions for the different polymers, where polymers were heated up to 800^oC at a constant heating rate of 4^oC/min, the atmosphere was adjusted in order to run the analysis under nitrogen flow (N_2, 99.999%)

2.2.3.2 Differential Scanning Calorimetry (DSC)

Differential scanning calorimetry device that was used is *DSC 204 F1 Phoenix*® (NETZSCH group – Germany). The analysis was performed for the samples AP1 and AP3, which are the polymers of interest according to the results we obtained from the surface area measurements as will be discussed in the next section. The measurements were done using the same heating parameters and ranges and number of cycles in order to obtain consistent and comparable data. Heating rate was set to be (10^oC/min.), in the range of 0^oC up to 500^oC and two different cycles were applied on each sample. DSC analysis data presented here was obtained as a second cycle measurement, in the first cycle the material was heated form the room temperature to 120°C and remained at an isotherm for 3 minutes then cooled back to 0°C and that's where the first cycle ends. The objective of the first cycle is to get rid of any residual solvent molecules or any adsorbed humidity that may

result in false transitions that did not arise from the material itself, and it also serves as an adjustment and conditioning for the material before getting to data acquisition cycle.

DSC is very helpful tool in determining the level of curing or crosslinking in the materials and this is the main objective here, and as we can see in the data given in (**Figure 9**), the materials show only exothermic transitions with no endothermic glass transitions, and this can be taken as a solid indication of the crosslinking property of the material, since it goes to decomposition directly. It can also be noticed that both the data obtained from the DSC analysis and the data from the TGA analysis, show consistency in the behavior as both of them indicate the same temperature region at which the decomposition of the materials take place.

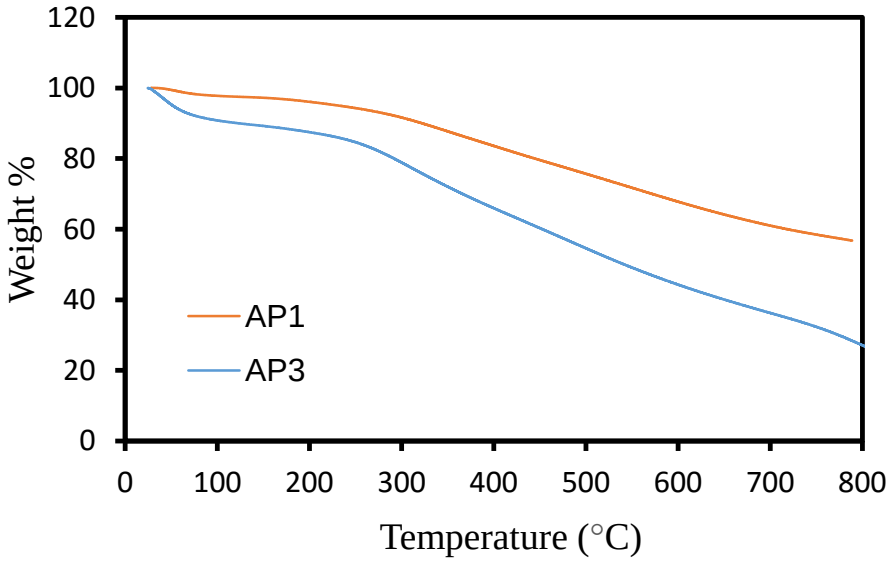

Figure 8 TGA for different AP polymers up to 800°C

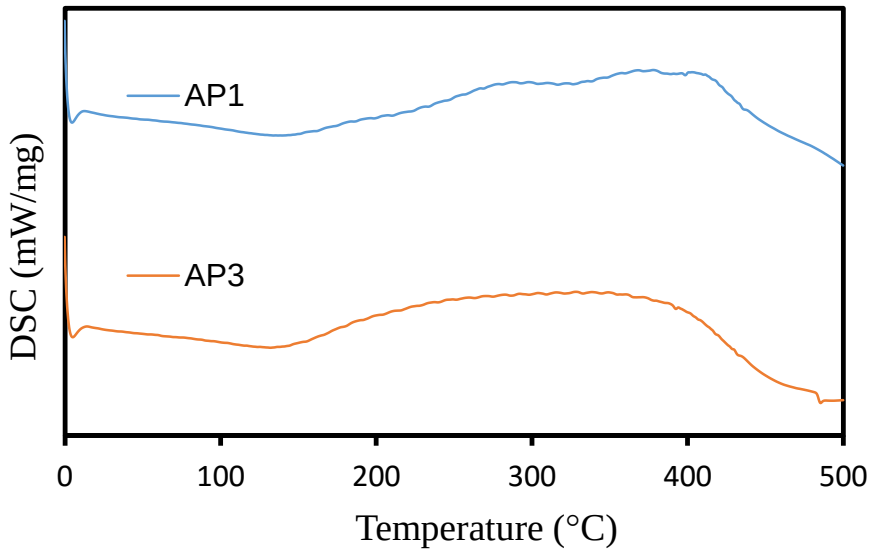

Figure 9 DSC data obtained for AP1 and AP3 polymers

The thermal stability of the polymers as shown in (**Figure 8**), shows that there is small loss stage in the low temperature region before 100°C in the polymers, which is back to the loss of gases or residual solvent molecules. Both of the polymers are showing almost total stability up to 250°C or a bit higher. The weight loss continues gradually without any sharp or distinguishable stages until they reach a residual mass percentage of around 60% and 30% for AP1 and AP3 respectively.

2.3 Gas Adsorption Calculations and Characterization

All gas uptake measurements were done on Quantachrome® Autosorb iQ instrument, isotherms were obtained at different temperatures mainly at 273K & 298K, 0°C & 25°C respectively, for Carbon Dioxide (CO_2, 99.9995%), Methane (CH_4, > 99.9%) and Nitrogen (N_2, 99.999%). Measurements for Nitrogen uptake at 77K were operated on Quantachrome® quadrasorb instrument using Nitrogen (N_2, 99.999%) and Helium (He, 99.99%) for refilling.

2.3.1 Isotherm characterization & Surface area

Surface area was measured for all the polymers from isotherms obtained under the same conditions (N_2 gas at 77K) using both BET (Burnauer–Emmett–Teller) and Langmuir models, and results are listed in (**Table 6**). According to the IUPAC technical report [25] published in 2015, the isotherms assigned to AP1, AP2 and AP4 that are shown in (**Figure 10**) are characterized as type I isotherms, this reflects a micropore nature of the materials. In normal type I isotherm the uptake of the gas increases steeply at very low pressures, this happens because of the adsorptive-adsorbent interactions in these small narrow micropores resulting in the filling of these pores at low relative pressure. After the steep uptake stage, type I isotherm normally reaches a limiting value of gas uptake, this value is not dependent on the total or the internal surface area of the material but on the accessible micropore volume. It's obvious that in our case the isotherms do not reach any limiting value instead they continuously increase, not only that but they go to sharp N_2 uptake at high relative pressure ($P/P_o > 0.9$), this condensation behavior may cause some confusion between these isotherms and the isotherms obtained from non-porous or macro-porous materials, Type II isotherms, but actually this behavior can be ascribed to the inter-particle voids condensation [26], since these materials are very fine they may aggregate and pack in order to produce a larger macro-pores [27] which was investigated by SEM imaging.

Isotherm assigned to $AP1_b$ shows very low surface area and odd zigzag behavior along the whole measured region, the general pattern of the experimental points shows Type II isotherm, and the material can be described as non-porous. We think that the data obtained for $AP1_b$ are not reliable for any further calculations or modeling. Hysteresis loops observed in the isotherms, except for $AP1_b$, can be assigned as type H3 loop especially for

AP2 that shows a typical loop. Type H3 is characterized by its resemblance to type II isotherm, and it can be caused by a non-rigid aggregates of particles or because of the presence of macro-pores in the network that are not completely filled [25].

2.3.2 Pore volume & Pore size distribution

As mentioned above, since the materials contain macro-pores, it causes steep rise in the nitrogen uptake at high relative pressure. The total pore volume calculation is well defined in cases where the material does not contain any macro-pores and the isotherm maintain almost complete horizontal behavior over a range of relative pressure. Since this is not the case, we preferred to calculate the micro-pore volume, Pore radius and Pore size distribution using Dubinin-Astakhov (DA) method. There is another method called Dubinin-Radushkevich (DR) that is used for large numbers of micro-porous materials but it fails to linearize the adsorption data for microporous materials with heterogeneous distributions[28]. The Dubinin-Astakhov equation was proposed to be as follows:

$$W = W_o \exp\left[-\left(\frac{-RT \ln {}^{p}/_{p_o}}{E}\right)^{n}\right] \quad (1)$$

where, W is weight adsorbed at P/P_o and T, W_o is total weight adsorbed, E is characteristic energy and n is non-integer value (typically between 1 and 3).

This equation is a generalized formula of Dubinin-Radushkevich (DR) equation in which ($n=2$), and as mentioned before it was found to be more suitable for fitting adsorption data for material of heterogeneous micropores[29]. The pore size distribution calculations were done using the same DA method, Non-Linear Density Functional Theory (NLDFT) and Quenched Solid Density Functional Theory (QSDFT) are used depending

on the knowledge of the pore structure and geometry in order to give reliable results, and this is why we were not able to use one of these methods since we know that the polymers are amorphous hyper-crosslinked and from the isotherm type we can judge that it contains different pore sizes and subsequently different geometries as discussed earlier in this section. So as we cannot, for sure, define the structure of the pores we decided that it is more suitable to use the DA method instead of the NLDFT or QSDFT methods.

Table 6 Surface Area of Different AP polymers using BET & Langmuir models

Polymer name	BET (m^2/g)	Langmuir (m^2/g)	Micropore volume[(a)] (cc/g)	Pore radius[(a)] (Å)
AP1	532	633	-	-
$AP1_a$	278	531	0.094	8.400
$AP1_b$	18	35	-	-
AP2	161	278	-	-
AP3	645	861	0.289	8.100
AP4	377	796	0.207	8.400

(a) Both micropore volume and pore radius were calculated using the Dubinin-Astakhov (DA) method.

Isotherm graphs of N_2 at 77K for polymers listed above are provided in (**Figure 10**) with the BET surface area for each polymer.

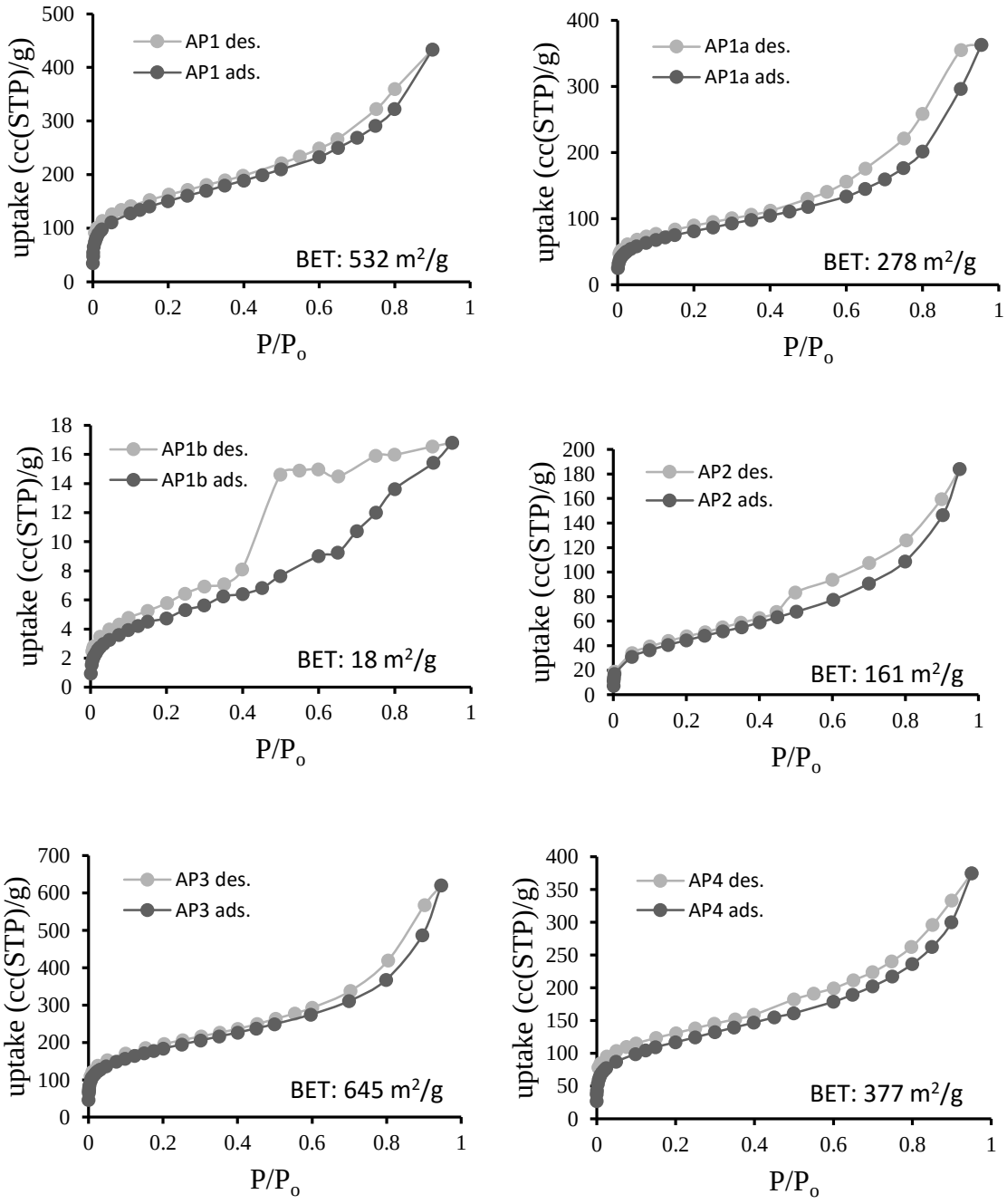

Figure 10 N_2 gas uptake at 77K for all AP polymers

2.3.3 Gas uptake measurement

Surface area measurements were taken in consideration in order to pick the polymers for the gas uptake measurements, since there is always relation between surface area and the uptake capacity of materials, the polymers with highest surface area were picked for application test, these polymers are **AP1** and **AP3**.

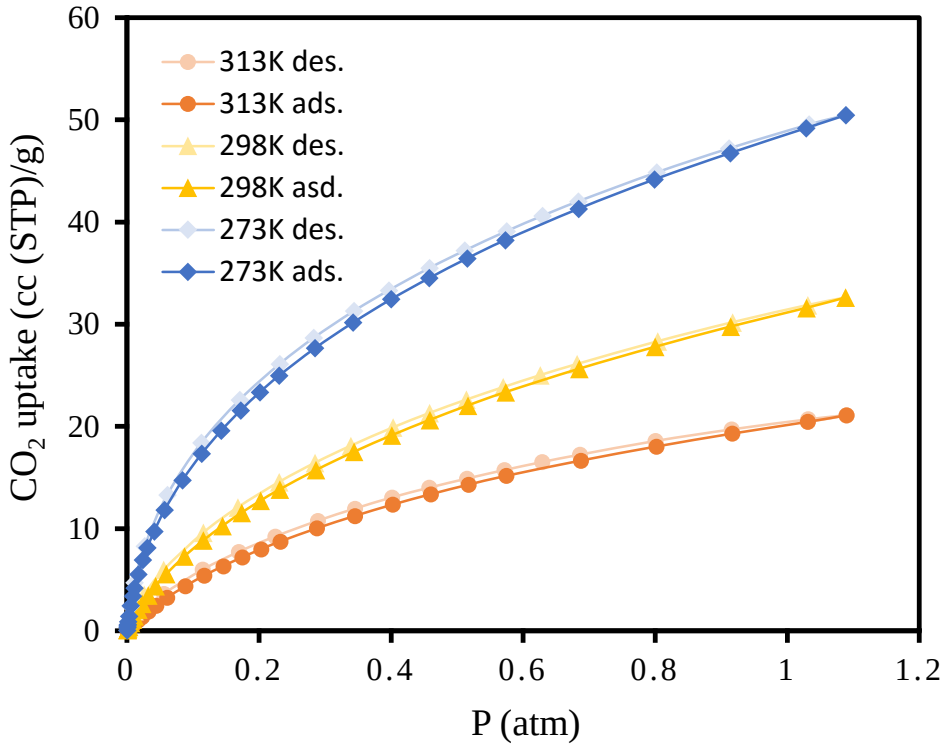

Figure 11 CO_2 gas uptake at different temperatures (273K, 298K & 313K) as measured for AP3 polymer. (rich colored) for adsorption, (faint colored) for desorption

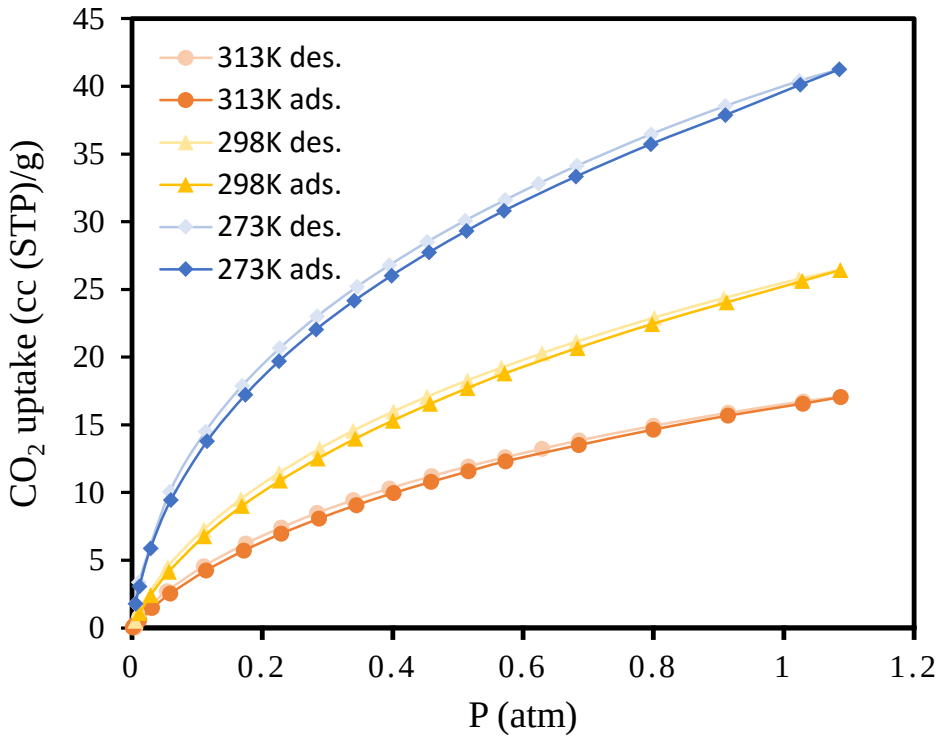

Figure 12 CO_2 gas uptake at different temperatures (273K, 298K & 313K) as measured for AP1 polymer. (rich colored) for adsorption, (faint colored) for desorption

From the data given in (**Figure 11** & **Figure 12**), it can be clearly decided that the AP3 scores higher CO_2 uptake not only at 273K (0°C) but at higher temperatures also, and that is why we gave it all the attention for the rest of study. AP3 achieved a CO_2 uptake of (50.5 cc/g ≡ 2.3 mmol/g) around 1 atm at 273K. For higher temperatures it reached (32.6 cc/g ≡ 1.5 mmol/g) and (21.1 cc/g ≡ 0.9 mmol/g) at 298K and 313K respectively at same pressure. To further investigate the gas uptake properties of AP3, it was subjected to gas uptake measurements on two other gases which are methane (CH_4) and nitrogen (N_2), these measurements were conducted in same pressure range but not for all temperatures.

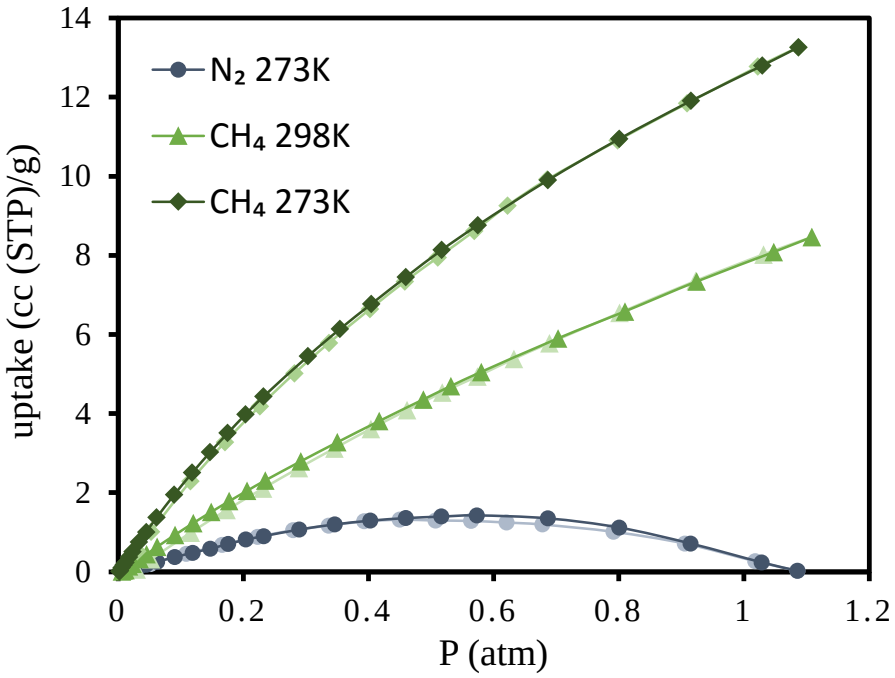

Figure 13 N_2 & CH_4 gases uptake at different temperatures for AP3 at 273K. (rich colored) for adsorption, (faint colored) for desorption

The methane uptake was measured at two temperatures 273K and 298K, but the nitrogen was only measured at 273K. As we can see in (**Figure 13**) nitrogen uptake undergoes strange behavior with very low uptake, this can be set back to the disability of the material to adsorb the gas at this temperature and so an immediate desorption behavior takes place. As this is the case at 273K and it is known that gas adsorption is inversely proportional with temperature and thus for nitrogen uptake the error most probably will increase with increasing the temperature only 273K nitrogen uptake was measured.

2.3.4 Selectivity measurements

selectivity of AP3 polymer for CO_2 gas was determined against two different gases, the nitrogen gas ($S_{CO2/N2}$) and the methane gas ($S_{CO2/CH4}$). The isotherms that were used are shown in (**Figure 14**). Isotherms of the three gases, CO_2, N_2 and CH_4, are measured at

273K in low pressure region. Initial slope selectivity and Henry's law selectivity methods were conducted using these measurements.

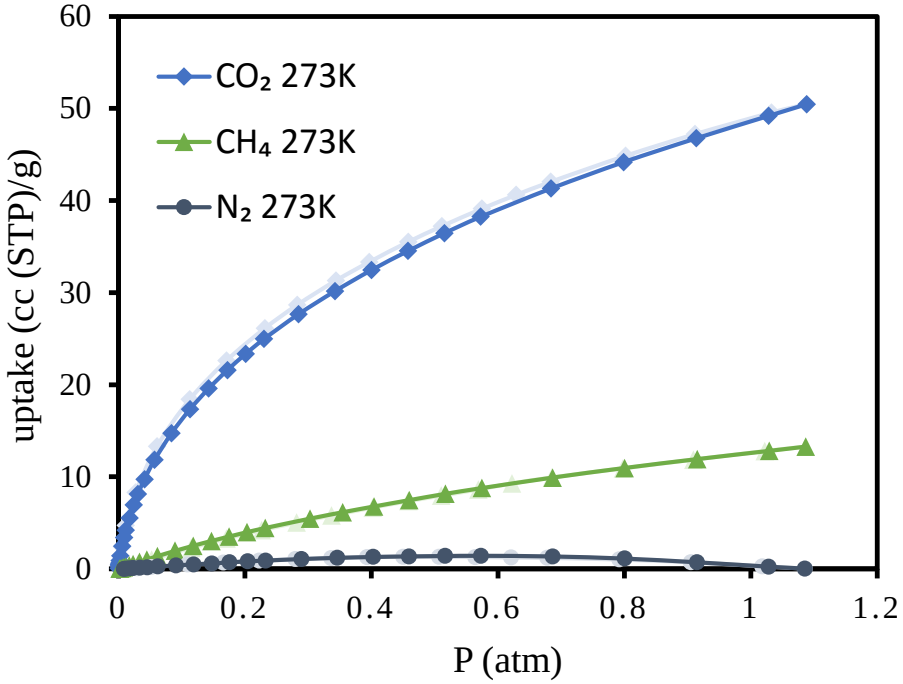

Figure 14 Isotherms for CO_2, N_2 and CH_4 gases at 273K, (rich colored) for adsorption, (faint colored) for desorption

2.3.4.1 Initial slope selectivity

It was calculated using the experimental data points provided in (**Figure 14**). This method depends on the linear behavior noticed in the isotherms that can be used to describe the affinity of a material towards a specific gas. So as the slope of an isotherm curve for certain gas in that linear region increases, it reflects a high affinity of the material towards this specific gas, since the uptake increases highly and vice versa. By comparing the slopes of different gases at same conditions we can then get an idea about the affinity of one material towards these gases. This method is actually based on the Henry's law, since it

describes the gas adsorption on solid as linear relation. The Henry's isotherm equation is [30]

$$q = kP \tag{2}$$

where, q is the adsorbed amount per unit weight of adsorbed gas (cc/g), P is the adsorbate gas pressure (torr), and K is the Henry's law constant (cc/g.torr).

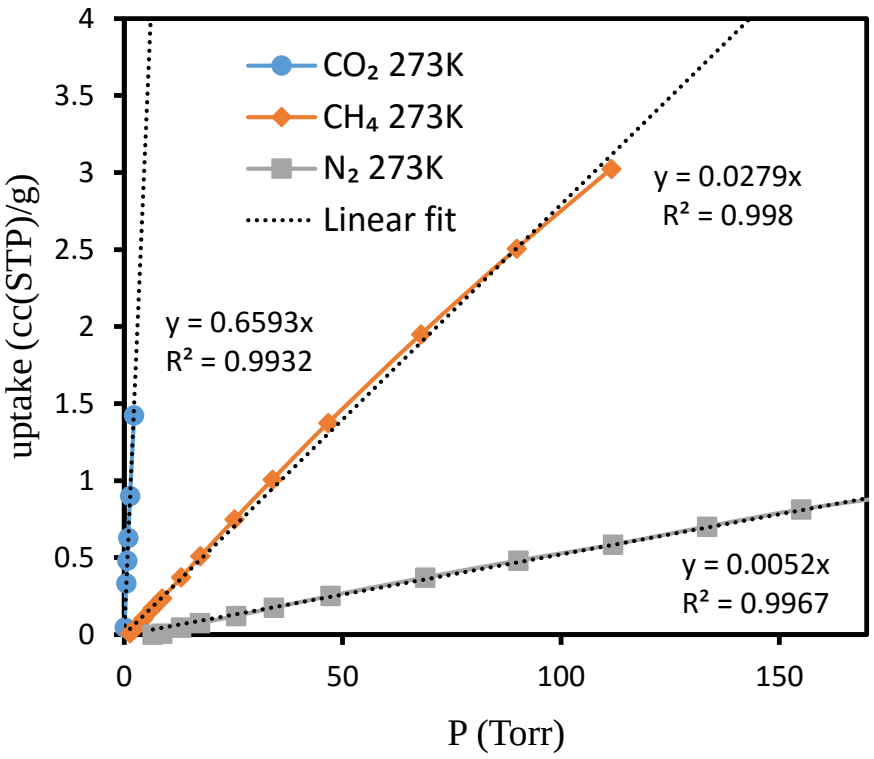

Figure 15 Adsorption selectivity of CO_2 over N_2 and CO_2 over CH_4 as calculated by the initial slope method

Depending on the data provided in (**Figure 15**) the selectivity can be given by dividing the slopes of the gases to be studied as shown in (equation 3).

$$S_{a/b} = \frac{K_a}{K_b} \quad (3)$$

where, *a* and *b* represent the higher and lower gas in its affinity toward the material respectively. K_a and K_b are Henry's constants for gases *a* and *b* respectively.

All the data for the formerly mentioned selectivity calculation are tabulated in (Table.3)

Table 7 Parameters for initial slope selectivity for CO_2, CH_4 and N_2 gases

Gas type	Equation	CC (R^2)	Slope	Intercept
CO_2	y= K_a*x	0.9932	0.6593	0
CH_4	y= K_b*x	0.9980	0.0279	0
N_2	y= K_c*x	0.9967	0.0052	0

Selectivity CO_2/CH_4	23	Selectivity CO_2/N_2	126

2.3.4.2 Henry's Law selectivity

It was measured after fitting the different single-component gas isotherms of CO_2, CH_4 and N_2 at 273K with different models seeking the best fitting model since the data must be fitted precisely. The model that was found to best fit the isotherms is the dual-site Langmuir model [31], and the equation for this model is (equation 4)

$$q = q_{m1}\frac{a_1 P}{1 + a_1 P} + q_{m2}\frac{a_2 P}{1 + a_2 P} \quad (4)$$

where, *q* is the adsorbed amount of gas per mass of adsorbent material (mmol/g), *P* is the pressure of the bulk gas at equilibrium with the adsorbed phase (Torr), q_{m1} and q_{m2} are the

saturation capacities of sites 1 and 2 (mmol/g), a_1 and a_2 are the affinity coefficients of the sites (1/Torr).

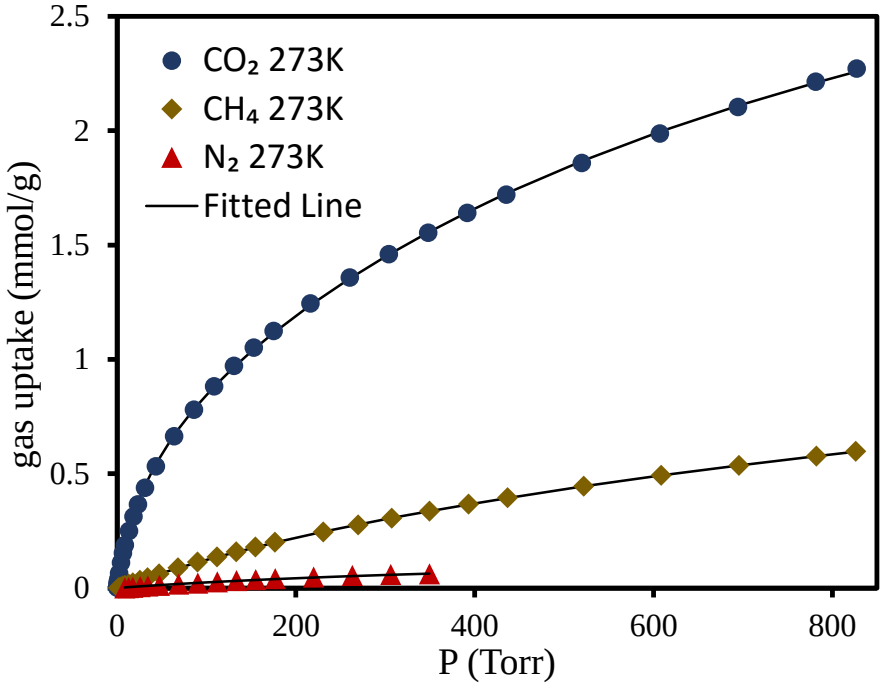

Figure 16 AP polymer fitting curves of single-component isotherms as measured using the dual-site Langmuir model

It is important to clarify that because of the odd behavior of N_2 isotherm that was discussed earlier, we used only the region in the isotherm that shows normal increasing in uptake with pressure, and neglected the part with the unusual decreasing behavior since it will not fit with any fitting model and will just increase the error dramatically. Depending on the fitting parameters obtained from the equation, the Henry's constant is calculated from the saturation capacity (q_m) and affinity coefficient (a) for each gas independently, using the following equation

$$S_{a/b} = \frac{K_a}{K_b} = \frac{(q_{m1} * a_1 + q_{m2} * a_2)_a}{(q_{m1} * a_1 + q_{m2} * a_2)_b} \quad (5)$$

The fitting parameters for these isotherms as calculated by the dual-site Langmuir model and the selectivity calculation is recorded in (**Table 8**)

Table 8 Fitting parameters for CO_2, CH_4 and N_2 single-component isotherms at 273K as fitted by dual-site Langmuir model

Parameter	CO_2	CH_4	N_2
q_{m1}	3.34167	0.32985	0.08439
q_{m2}	0.64755	1.67540	0.09172
a_1	0.00116	0.00255	0.00162
a_2	0.03335	0.00035	0.00162
K_H	0.02546	0.00142	0.00029
error	0.00139	0.00002	0.00003

Selectivity CO_2/N_2	89	Selectivity CO_2/CH_4	18

2.3.5 Estimation of Isosteric Heat of Adsorption (Q_{st})

The Q_{st} defines the affinity and the energy of the adsorption between the gas molecules and adsorbent material. This property is intrinsic for a material and does not change with changing the temperature. A virial-type expression comprising temperature independent parameters a_i and b_j was used in order to relate between two different single-component isotherms of CO_2 gas at two different temperatures (273K and 298K). The virial-type equation used is [32]

$$ln(p) = \ln(v) + \frac{1}{T}\sum_{i=0}^{m}\left(a_i v^i\right) + \sum_{i=0}^{n}\left(b_i v^i\right) \quad (6)$$

where, P is pressure (Pa), υ is the adsorbed amount (mol/g), a_i and b_j are the virial coefficient, T is temperature, and m and n represent the number of coefficients required to adequately describe the isotherms, these two numbers (m and n) should be kept as minimum, i.e. they were increased gradually up to a certain limit at which any additional coefficients will not cause any significant improvement on the fit.

After applying the fitting equation, the fitted lines must be evaluated for their eligibility to make sure that the resulting data are reliable, and for that the error must be calculated as indicated in this equation

$$\sigma^2 = \left({}^{1}/_{N}\right)\sum_{j=1}^{N}\left(\ln p_j^{exp} - \ln p_j^{eq}\right)^2 \tag{7}$$

where, σ^2 is error of fitting value of ln (p), N is number of experimental points, $ln\ p_j^{exp}$ and $ln\ p_j^{eq}$ are the pressure natural logarithms of the experimental and equation fitted data respectively.

Only the values of the a_i virial coefficient, from a_o up to a_m, used in the fitting were used in the calculation of the isosteric heat of adsorption using the following equation

$$Q_{st}(\upsilon) = -R\sum_{i=0}^{m}\left(a_i \upsilon^i\right) \tag{8}$$

where, Q_{st} is the isosteric heat of adsorption for a specific gas uptake (kJ/mol), R is the universal gas constant (J/mol.K).

The onset isosteric heat of adsorption or the heat of adsorption at zero gas uptake (Q_o) can also be measured by reducing equation (8) to a simpler form in which it is not dependent on the uptake any more, by only using a_o virial coefficient in the calculation

$$Q_o = -Ra_o \tag{9}$$

The value of Q_o describes the binding affinity of a totally adsorbate-free material towards the gas molecule on its most active adsorption sites.

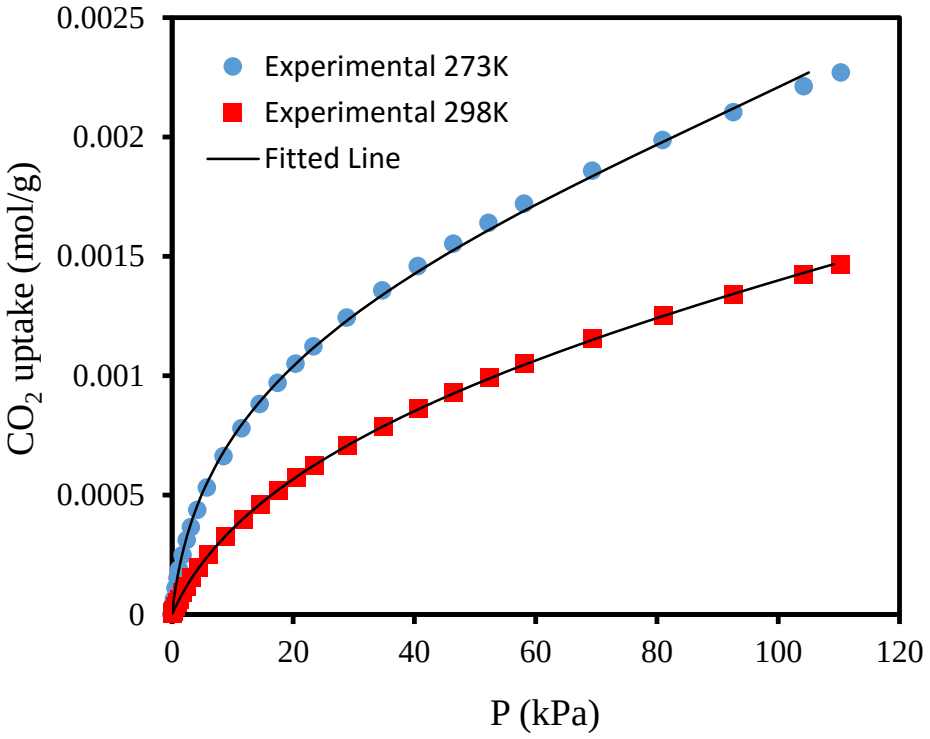

Figure 17 (AP3) polymer CO_2 isotherms at 273K and 298K of experimental (Markers) and fitted (black line) data obtained from the virial-type equation

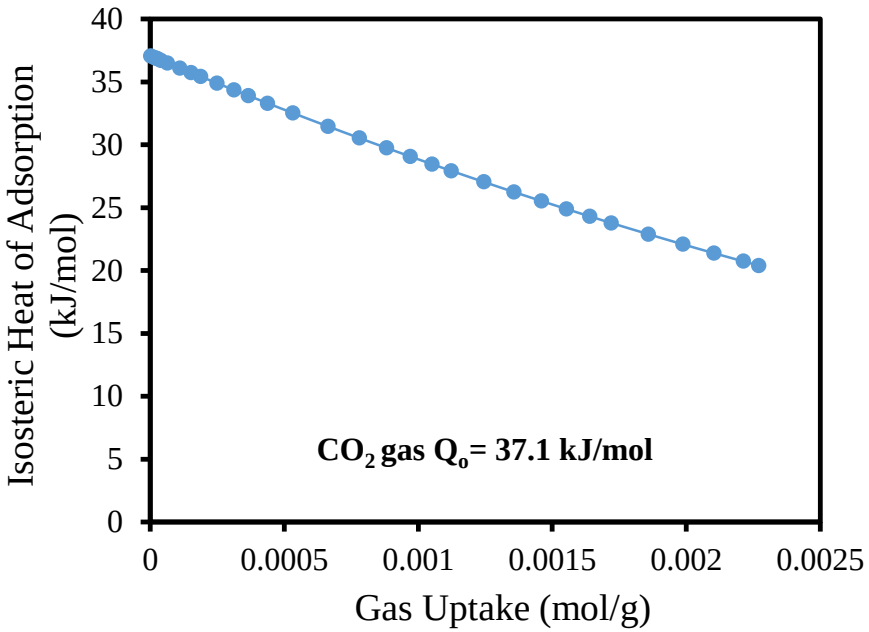

Figure 18 AP polymer Isosteric heat of adsorption curve of CO_2 gas as estimated form the virial-type equation

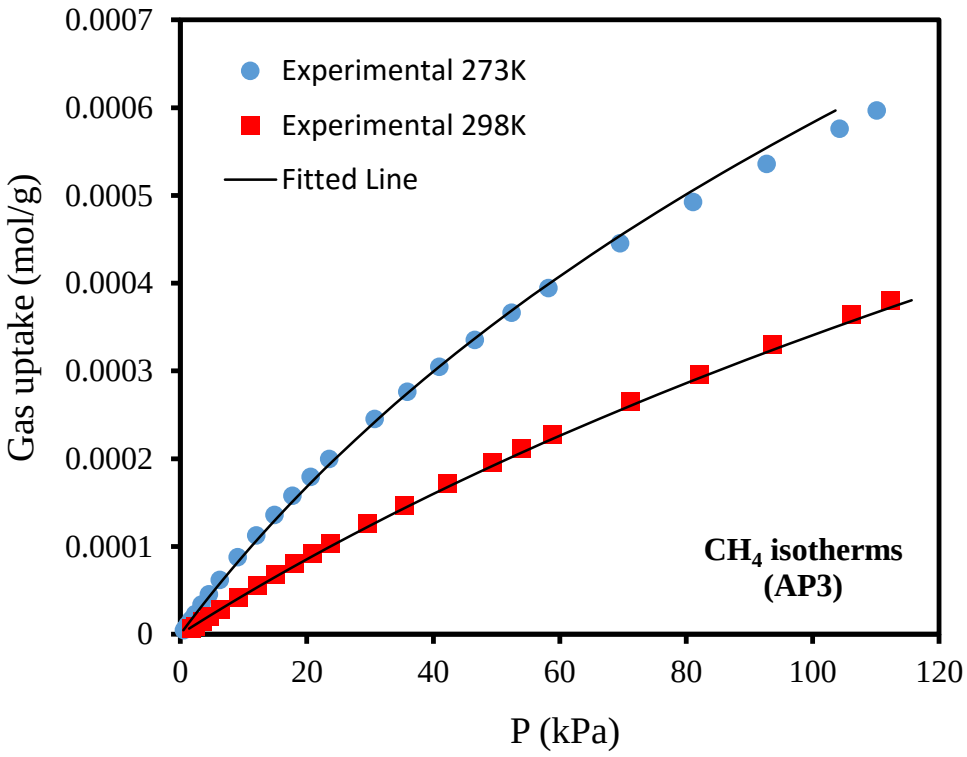

Figure 19 AP3 polymer CH_4 isotherms at 273K and 298K of experimental (Markers) and fitted (black line) data obtained from the virial-type equation

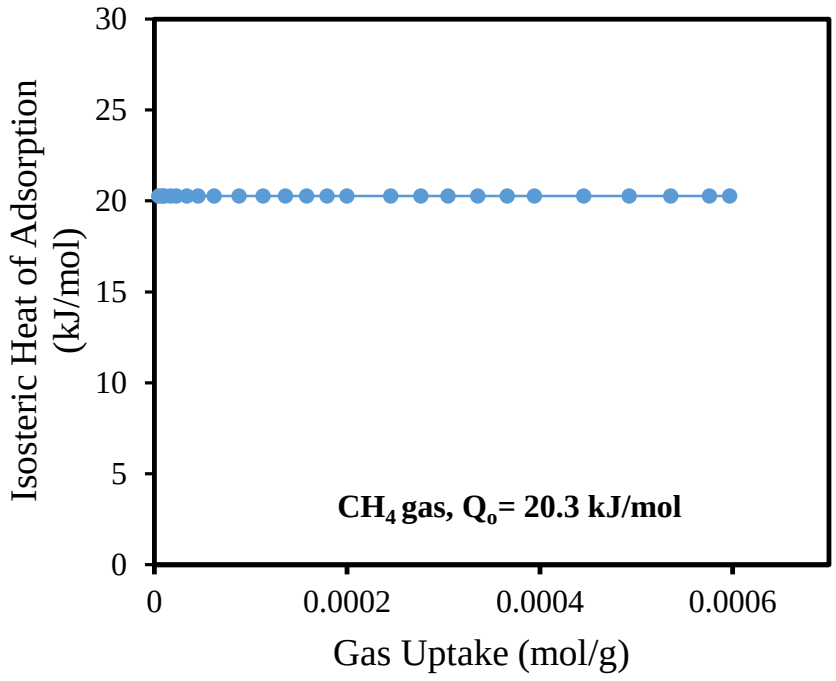

Figure 20 AP polymer Isosteric heat of adsorption curve of CH_4 gas as estimated form the virial-type equation

All fitting parameters data used for the calculation of the isosteric heat of adsorption for CO_2 and CH_4 gases are provided in (**Table 9**)

Table 9 All fitting parameters used in the virial-type equation fitting of CO_2 and CH_4 isotherms at 273K and 298K for AP3

Parameter	CO_2	CH_4
a_o	-4458.818996	-2439.202366
a_1	1073052.701	11.1458962
a_2	-83903957.61	-
b_o	31.63915917	27.38286366
b_1	-2200.619949	878.8926088
Error (σ^2)	0.0036	0.0043
Q_o (kJ/mol)	37.1	20.3

CHAPTER 3

FULL SERIES WORK

3.1 Introduction

Introduction of different functionalities and the study of their effect on the gas sorption is one of the main objectives of this work, and here in this chapter we are introducing polymers with heterocyclic moieties containing oxygen and sulfur atoms in our series. The full series is consisting of five polymers which are: Aniline-Pyrrole (AP), Aniline-Furan (AF), Aniline-Thiophene (AT), Pyrrole-Furan-Thiophene (PFT) and Pyrrole-Furan-Thiophene-Aniline (PFTA). Since the AP was already studied in Chapter 2, this chapter will discuss the synthesis of the other four polymers.

After the synthesis the characterization will be discussed as a comparison between the full series including the AP polymer (best polymer from chapter 2 (AP3)). Finally, the application of CO_2 sorption will be tested for the whole series then a detailed study for the best of them. We used the study we made on the Aniline-pyrrole polymers to further investigate the properties of this copolymerization condensation reaction between Aniline and the aforementioned five-membered heterocyclic rings and we found that the polymers show different behavior from what we accomplished with the AP. Of course we know that the three heterocyclic compounds Pyrrole, Furan and Thiophene are not identical in their properties and show different polarity and even aromaticity indices [33] as indicated by Bird Aromaticity index for heterocyclic compounds since it shows that the aromaticity indices (I_A) for Pyrrole, Furan and Thiophene are 85, 53 and 81.5 respectively. And also

the HOMA index [34] that also shows similar trend to that of Bird index and recorded 0.966, 0.656 and 0.873 for Pyrroles, Furans and Thiophenes respectively.

3.2 Synthesis

We followed the procedure that gave us the best AP polymer, and that was (AP3) (method number 3, see section 2.1.1.3) but the surface area of these polymers were very low that can be related to non-porous materials. So, the rest of the methods were also tried, some methods didn't give any stable insoluble product that can be separated, and since it was not the case for the AP it emphasized that using these synthesis routes induces different chemistry to take place with the Furan and Thiophene.

The method used for (AP4) (method number 4, see section 2.1.1.4) gave better results than that obtained from method number 3, still not comparable to what we achieved from AP, and the rest of the study was applied on those polymers. Pyrrole-Furan-Thiophene (PFT) and Pyrrole-Furan-Thiophene (PFTA) were synthesized using method number (3) and method number (4) and gave no significant differences in the results. The general reaction scheme for the preparation of AF and AT polymers is given below:

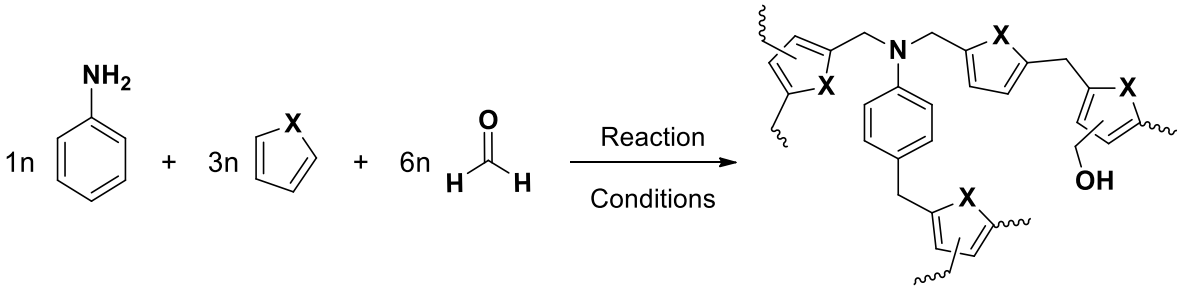

Figure 21 General reaction scheme for AF and AT polymer. x is O or S for Furan or Thiophene respectively

3.2.1 Reaction with Anhydrous Iron (III) Chloride ($FeCl_3$) Catalyst starting at Room Temperature (RT) and elevating gradually to (90ºC) in DMF solvent & N_2 atmosphere.

All chemicals were used as received without any extra treatment or purification. For this reaction $FeCl_3$ was first treated to make sure it's anhydrous, (20 g) of the $FeCl_3$ were added to a round bottom flask and mixed with (50 ml) $SOCl_2$ and kept under reflux for 2 hours, then dried under vacuum and stored under nitrogen as iron-black powder with green iridescence.

This reaction was performed under nitrogen atmosphere, so except for the solids monomers and solvent were added after reaction flask was filled with nitrogen. First, paraformaldehyde (0.06 mol) and anhydrous $FeCl_3$ were added and flask was then sealed with a septum. After replacing the air in the flask with nitrogen, DMF (10 ml) was added followed by addition of Aniline (0.01 mol) and Furan or Thiophene (0.03 mol) simultaneously. Reaction starts and proceeds 6-7 hours at room temperature, then it is introduced to oil-bath adjusted at 50ºC until it completes 24 hours from the beginning of the reaction. Finally, the temperature was elevated to 90ºC for about 4 hours.

The elementary analysis for the AF polymer was found C, 74.5; H, 6.3; N, 9.4 and for the AT polymer C, 71; H, 7.2; N9.2; S, 0.6.

After the solid was obtained from reaction vessel, the solid is treated with different solvents in order to get rid of all unreacted material and to replace the solvent used in the synthesis with a lighter solvent to obtain a pure solid as much as possible. The solid is then dried under vacuum for several hours (6-7 hrs.) at 70°C.

Table 10 Experimetnal details of AF and AT polymers

(AF)				
Reaction vessel components				
Aniline (0.01 mol)	Furan (0.03 mol)	Paraformaldehyde (0.06 mol)	DMF	Anhydrous $FeCl_3$ (0.006 mol)
0.96 g	2.03 g	1.80 g	10 ml	0.95 g
Temperature: RT-50 -80°C		Time: 28-30 hours		Yield: 31%
Trituration: Methanol → Diethyl ether → Ammonia soln. → Distilled water → Methanol **(Sonication is used)**				
(AT)				
Reaction vessel components				
Aniline (0.01 mol)	Thiophene (0.03 mol)	Paraformaldehyde (0.06 mol)	DMF	Anhydrous $FeCl_3$ (0.006 mol)
0.91 g	2.18 g	1.81 g	10 ml	0.97 g
Temperature: RT-50 -80°C		Time: 28-30 hours		Yield: 34%
Trituration: Methanol → Diethyl ether → Ammonia soln. → Distilled water → Methanol **(Sonication is used)**				

The reaction scheme for PFT polymer is given below:

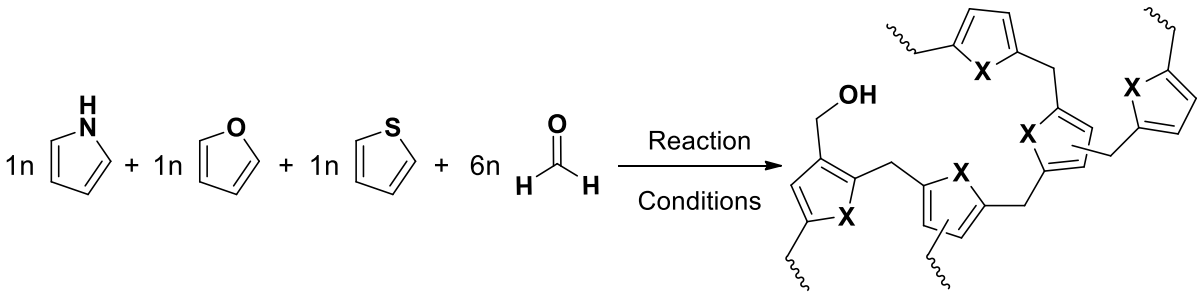

Figure 22 Reaction scheme for the PFT polymer. x is NH, O or S for pyrrole, furan or thiophene respectively

The reaction scheme for PFTA polymer is given below:

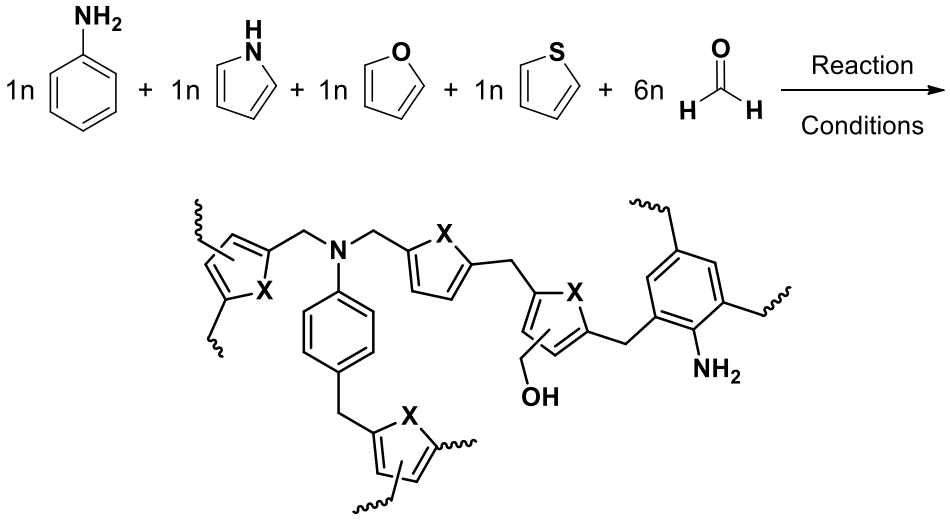

Figure 23 Reaction scheme for the PFTA polymer. x is NH, O or S for pyrrole, furan or thiophene respectively

The procedure for these two reactions, PFT and PFTA, are exactly the same as described for AF and AT polymers but differing in the quantities and molar ratios as indicated in the reaction schemes and also in summary tables below. The elementary analysis for PFT polymer was found C, 64.8; H, 7.4; N, 10.26 and for PFTA polymer C, 66.7; H, 5.2; N, 10.3.

Table 11 Experimental details of PFT and PFTA polymers

<table>
<tr><th colspan="6">(PFT)</th></tr>
<tr><th colspan="6">Reaction vessel components</th></tr>
<tr><td>Pyrrole
(0.01 mol)</td><td>Furan
(0.01 mol)</td><td>Thiophene
(0.01 mol)</td><td>Formaldehyde
(0.06 mol)</td><td>DMF</td><td>Anhydrous $FeCl_3$
(0.006 mol)</td></tr>
<tr><td>0.7 ml</td><td>0.7 ml</td><td>0.8 ml</td><td>1.806 g</td><td>10 ml</td><td>0.97 g</td></tr>
<tr><td colspan="2">Temperature: RT-50 -80°C</td><td colspan="3">Time: 28-30 hours</td><td>Yield: 50%</td></tr>
<tr><td colspan="6">Trituration: Methanol → Diethyl ether → Ammonia soln. → Distilled water → Methanol
(Sonication is used)</td></tr>
</table>

(PFTA)						
Reaction vessel components						
Aniline (0.01 mol)	Pyrrole (0.01 mol)	Furan (0.01 mol)	Thiophene (0.01 mol)	Formaldehyde (0.09 mol)	DMF	Anhydrous $FeCl_3$ (0.009 mol)
0.9 ml	0.7 ml	0.7 ml	0.8 ml	2.71 g	10 ml	1.57 g
Temperature: RT-50 -80°C			Time: 28-30 hours			Yield: 56%
Trituration: Methanol → Diethyl ether → Ammonia soln. → Distilled water → Methanol **(Sonication is used)**						

3.3 Characterization

It is highly important before the beginning of the discussion in this section to denote that a lot of comparison will be held between the polymers and the notation will be written abbreviated as given in the last section, in the first part where the comparison was between AP polymers only, the polymers were given numbers to differentiate between them. In the sake of the simplicity we will denote the (AP3) polymer in this section as only (AP), since it is the only polymer of interest among the other Aniline-Pyrrole polymers

3.3.1 Nuclear Magnetic Resonance (^{13}C-NMR)

^{13}C-NMR spectra of the polymers were all taken at spin rate of 10 kHz and all the conditions are exactly the same as described earlier (see section 2.2.1). The spectra shown below are for the five polymers and for clarification, the peaks of AP, AF and AT polymers are compared with each other on simple structures represent the most common linkages as proposed from the spectra.

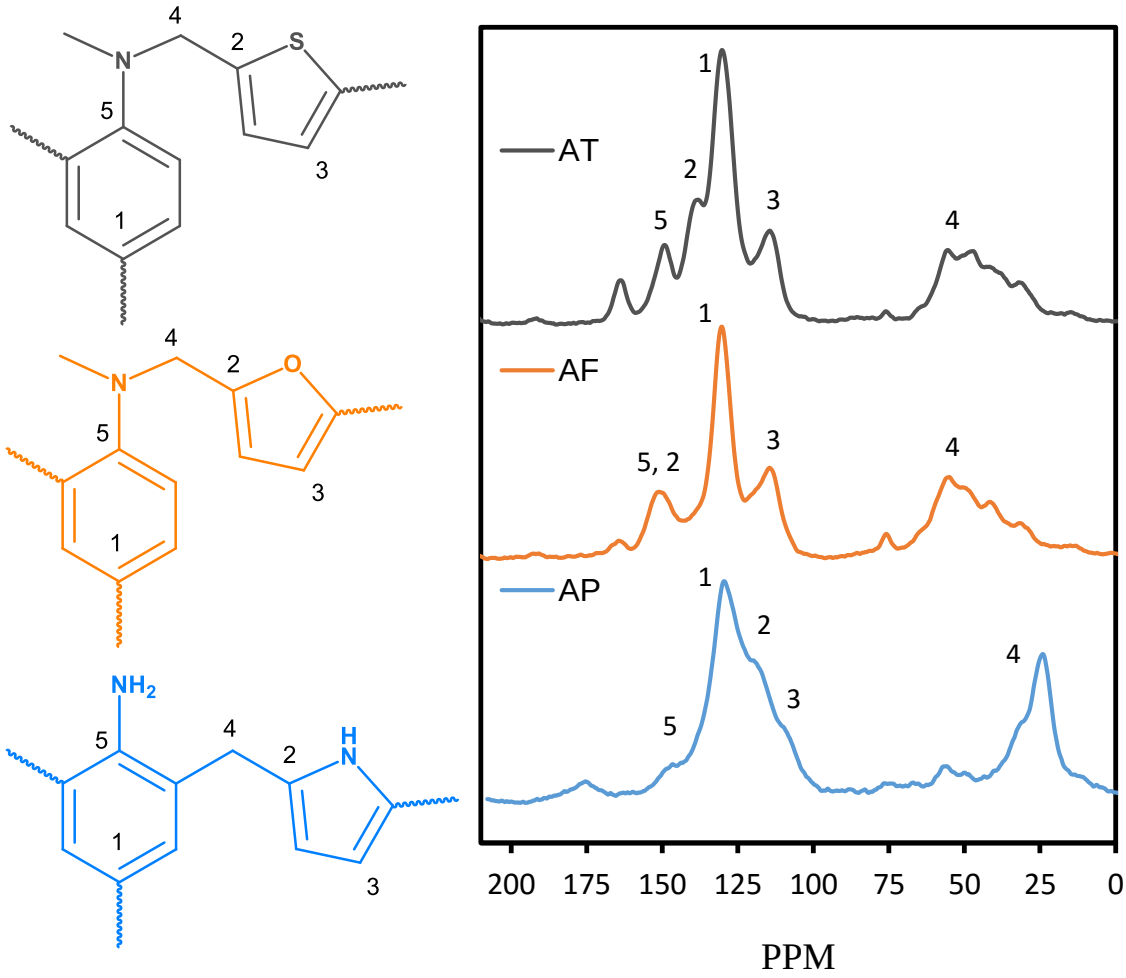

Figure 24 ^{13}C-NMR spectra for AP, AF and AT polymers

Each of the spectra shown above can be divided into two regions, aliphatic and aromatic. Aliphatic peaks in AP show a chemical shift around 25 ppm and proposed to represent the methylene carbon between rings as indicated in the structure, and it differ from the multi-peak shown for AF and AT which goes up to 52 ppm and proposed to be mainly from the attachment of methylene carbon to nitrogen of aniline. In the aromatic region a lot of differences can be detected but one broad peak can be found to constant in the three spectra which is peak number 1 and it was assigned to carbons of Aniline ring [35], carbons number 2 are appearing with different chemical shifts because of the effect

of the directly attached heteroatom with chemical shifts of 128, 151 and 140 ppm for pyrrole, furan and thiophene respectively [15], [36].

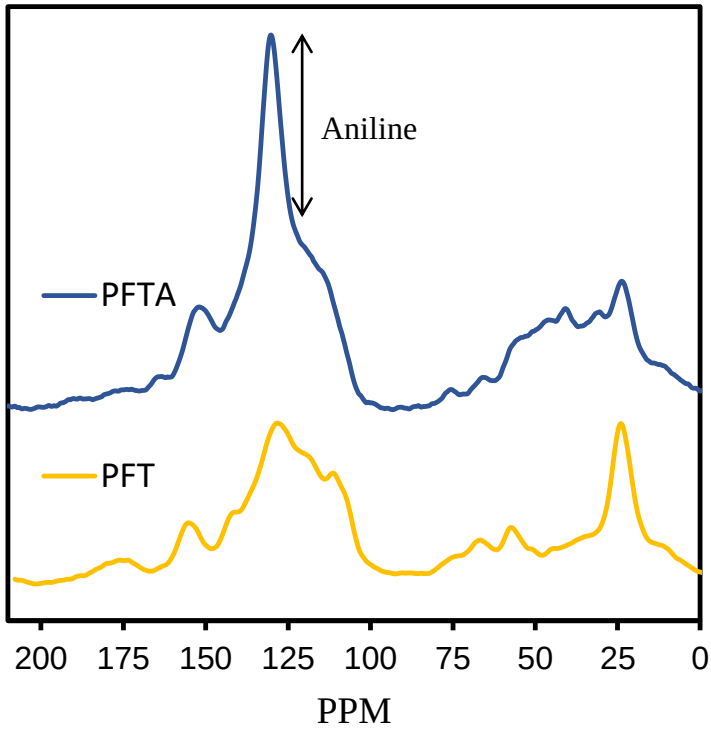

Figure 25 ^{13}C-NMR spectra for PFT and PFTA polymers

Spectra in (**Figure 25**) show a very broad hump in the aromatic region, this was expected as both polymers have three to four different aromatic monomers, the main difference between these two polymers lies in the introduction of aniline moiety in PFTA polymer and it is clear in the spectra as indicated by highly intense peak of aniline around 130 that was identified before. The aliphatic region in PFT show mainly one peak around 25 ppm since the methylene carbons are all proposed to link from rings with no direct heteroatom linking, which is not the case after the incorporation of Aniline in the PFTA polymer as aniline may attack the formaldehyde and link directly to the methylene carbon as discussed before.

3.3.2 Fourier Transform Infrared Spectroscopy (FTIR)

The solid state Infrared spectra were investigated for the detection of functional groups All the data were obtained using a *Perkin Elmer 16F PC FTIR* spectrometer using solid potassium bromide (KBr) pillets in a region of 4000-400 cm^{-1} (mid-IR region).

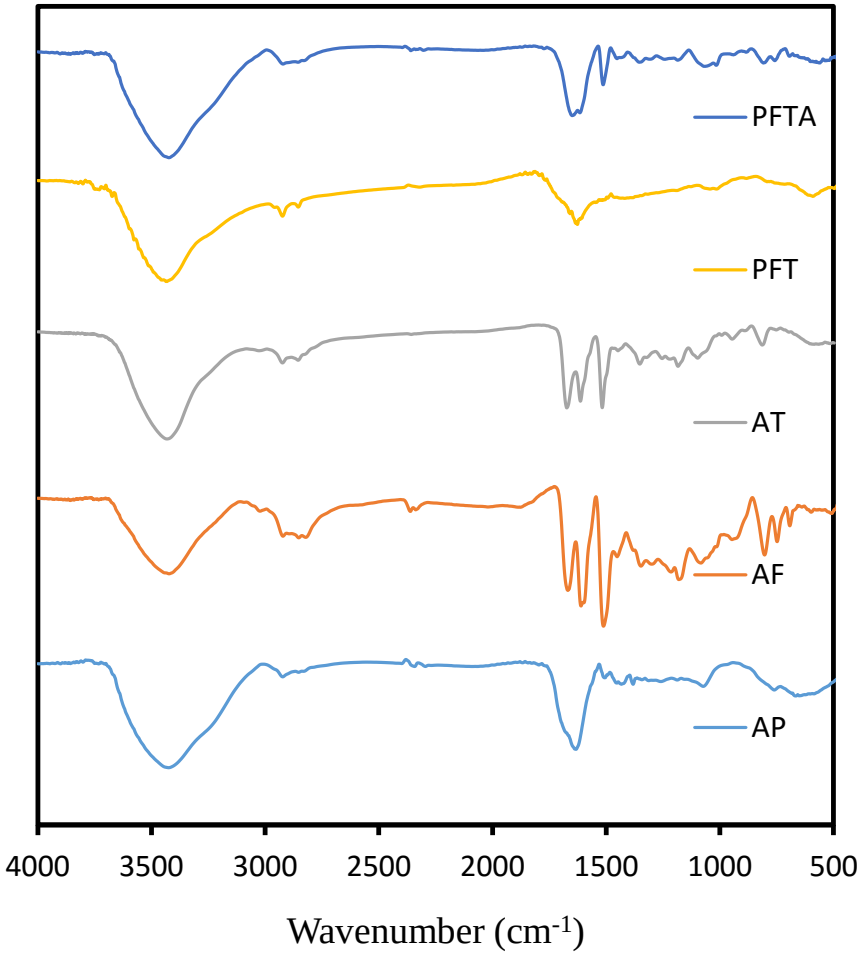

Figure 26 FT-IR spectra of all the polymers

Some of the AP polymer bands were elucidated in Chapter 2 (see section 2.2.2), so we will pay attention to the AF and AT now. For AF the spectrum shows the amine stretch of the aniline group and in the region of 1300 cm^{-1}, peaks at 3160 cm-1 is for C-H in furan

ring, 1510 cm^{-1} is for C=C in furan ring, two peaks at 1255 and 1313 cm^{-1} are assigned to the C-O stretch, and the peak at 752 cm^{-1} is for the mono-substituted furan ring [37].

For AT polymer, the following are the most distinguishable bands, the region of 1600 cm^{-1} is characteristic to C=C of the aromatic ring, the most characteristic peaks for sulfur compounds are observed in the spectrum, C-S stretch at 690 cm^{-1} and C=S stretch in the region of 1030–1275 cm^{-1} can be also observed and the 1434 cm^{-1} peak is a ring vibration that consists primarily of the symmetric stretching of the C=C bonds of thiophene.[38]. The bands in the PFT and PFTA are not so clear but they appear to be a combination of aforementioned bands of AP, AF and AT since the contain the same functionalities without any introduction of new monomers.

3.3.3 X-Ray Photoelectron Spectroscopy (XPS)

The XPS data were collected using *Thermo Scientific™ ESCALAB™ 250Xi X-ray Photoelectron Spectrometer*. The main objective from using XPS was to investigate the nature of the amine group in the polymers as primary, secondary or tertiary amine as the different states of amine groups are reported to have different binding energies that can be identified from the spectra [39], this can help in determining whether we have an exclusive linkage from the amine of the aniline or we have a free primary amine with linkages mainly produced from the aniline aromatic ring or that we have a mixture of these possibilities.

The data were obtained for the whole series, and in all of the spectra the binding energy scale was calibrated by setting the C 1s core level main peak or adventitious carbon at 284 eV. Polymers were found to cover the range from around 397 to 401 eV in the N 1s region, and according to literature and as indicated in (**Figure 27**).

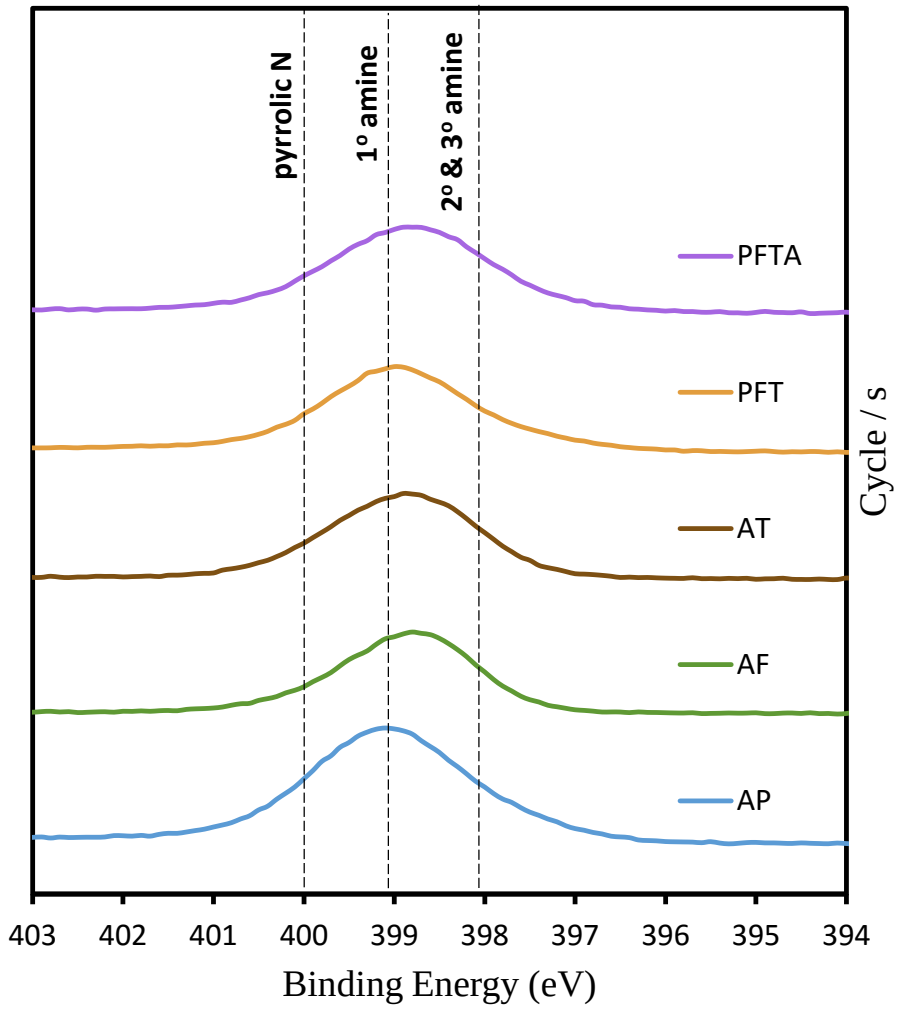

Figure 27 XPS spectra of the whole series for (N 1s)

Pyrrolic nitrogen appears at around 400.35 ± 0.3 eV, primary amine appears at 399.17 eV [40] and secondary and tertiary amines were reported to appear at similar binding energy of 398.07 eV [41], spectra show that the polymers cover the region of these binding energies with some differences caused by different intensities and contribution from these moieties in each polymer. In AP polymer the N 1s peak appears to be shifted to higher binding energy compared to the others, this may be because of the higher ratio of pyrrolic nitrogen and the assumption made earlier, depending on the ^{13}C-NMR spectrum,

that the main linkages in the AP polymer are from the aniline ring resulting in free primary amine.

XPS survey measurements for total binding energy region from 0 up to 1300 eV were investigated and showed only the elements of carbon, nitrogen, oxygen and sulfur with no any remaining residuals of iron or chloride ions left in the material from the anhydrous iron (III) chloride that was used as activating reagent in the reactions.

3.3.4 Thermal Properties

3.3.4.1 Thermal Gravimetric Analysis (TGA)

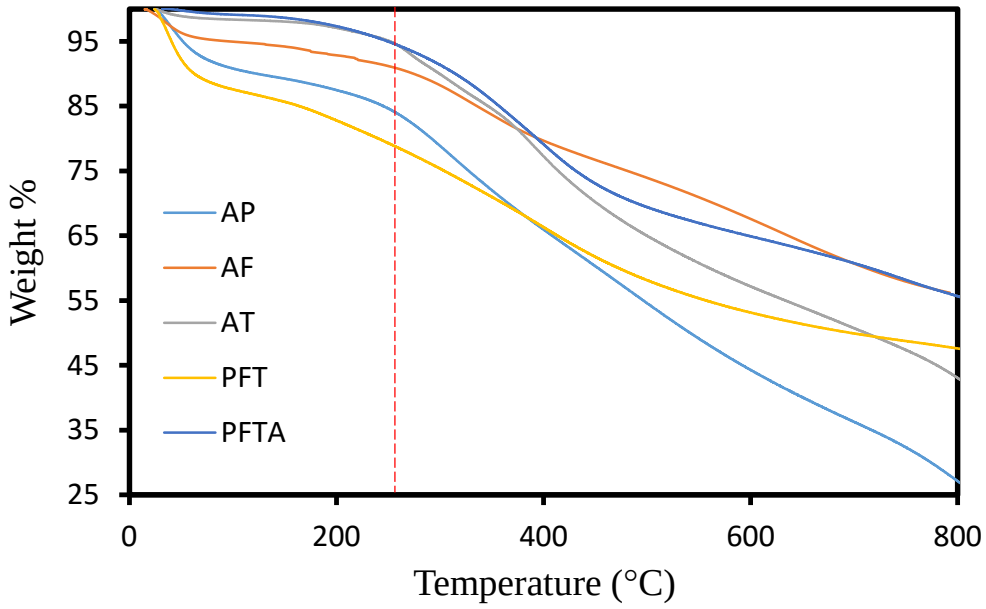

Figure 28 TGA comparison for all the polymers

Polymers were investigated for their thermal stability under nitrogen atmosphere with heating up to 800°C and as indicated by the dashed line in (**Figure 28**) the material show stability up to around 250°C, beside that most of the polymers does not show

complete decomposition and some, AF and PFTA, end up with residual mass percentage of 60%, and this behavior is attributed to the carbonization of the material [42].

3.3.4.2 Differential Scanning Calorimetry (DSC)

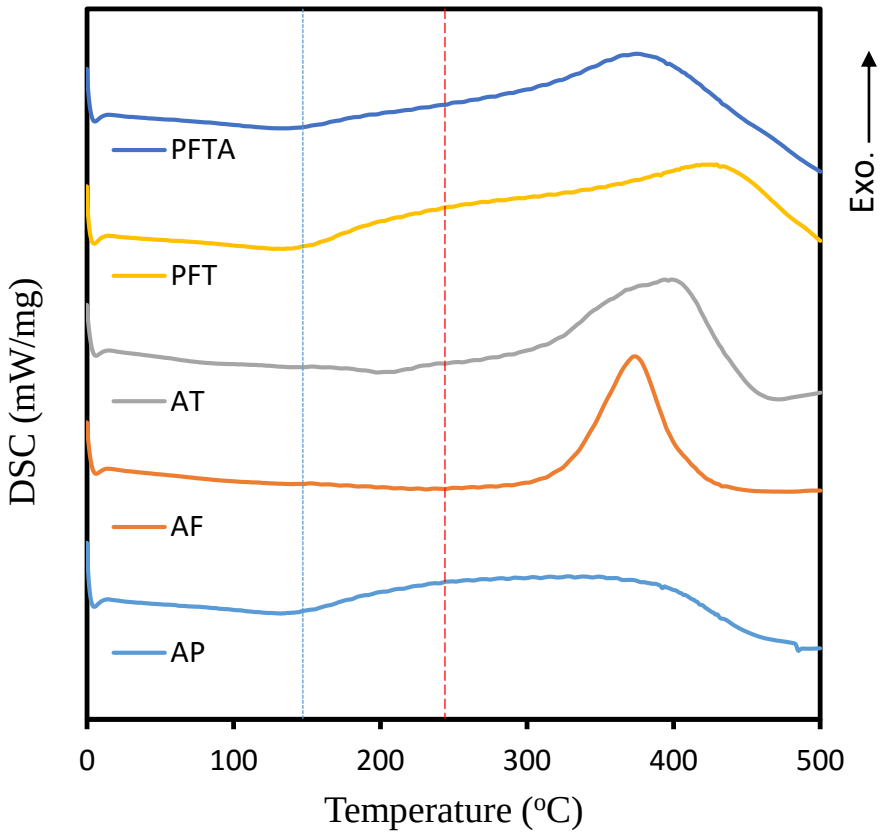

Figure 29 DSC graphs for All the polymers

DSC graphs show that all the polymers show high crosslinking property as there is no any indication of any endothermic behavior like melting or glass transition. As the decomposition was found to start around 250°C from the TGA, an exothermic transition can be indicated below this temperature around 150°C as indicated with (dotted line) and this transition attributed to crystallization or chain rearrangements and it is clear especially in the pyrrole containing polymers as shown in (**Figure 29**).

3.3.5 Powder X-Ray Diffraction (PXRD)

Powder X-Ray Diffraction was done for all the polymers to evaluate the amorphousity or crystallinity of the materials. The data was obtained in the range of 5 to 50 degrees with a rate of 2 degrees/min. From the data obtained and presented in (**Figure 30**) it can be clearly stated that all the synthesized polymers are amorphous in nature with no indication of any crystallinity, and this was highly expected since the polymers have high degree of cross linking according to what we got from the DSC analysis.

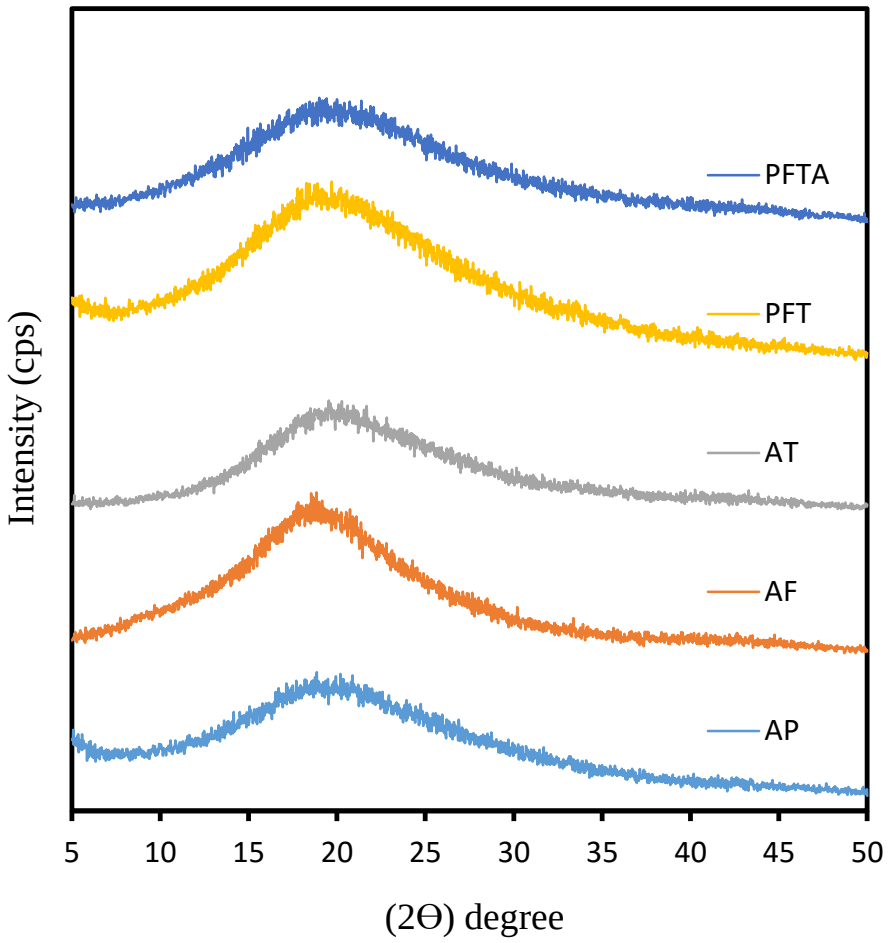

Figure 30 Powder XRD comparison for all the polymers

3.3.6 Scanning Electron Microscope imaging (SEM)

The SEM images were captured on *LYRA3 TESCAN* instrument, all the materials were coated using gold coating of thickness 10 nm directly before being introduced to the machine. The parameters used for these images are listed below:

SEM HV: 20.0 kV, WD: 9.82 mm, SEM MAG: 50.0 kx and view field: 5.78 micrometer.

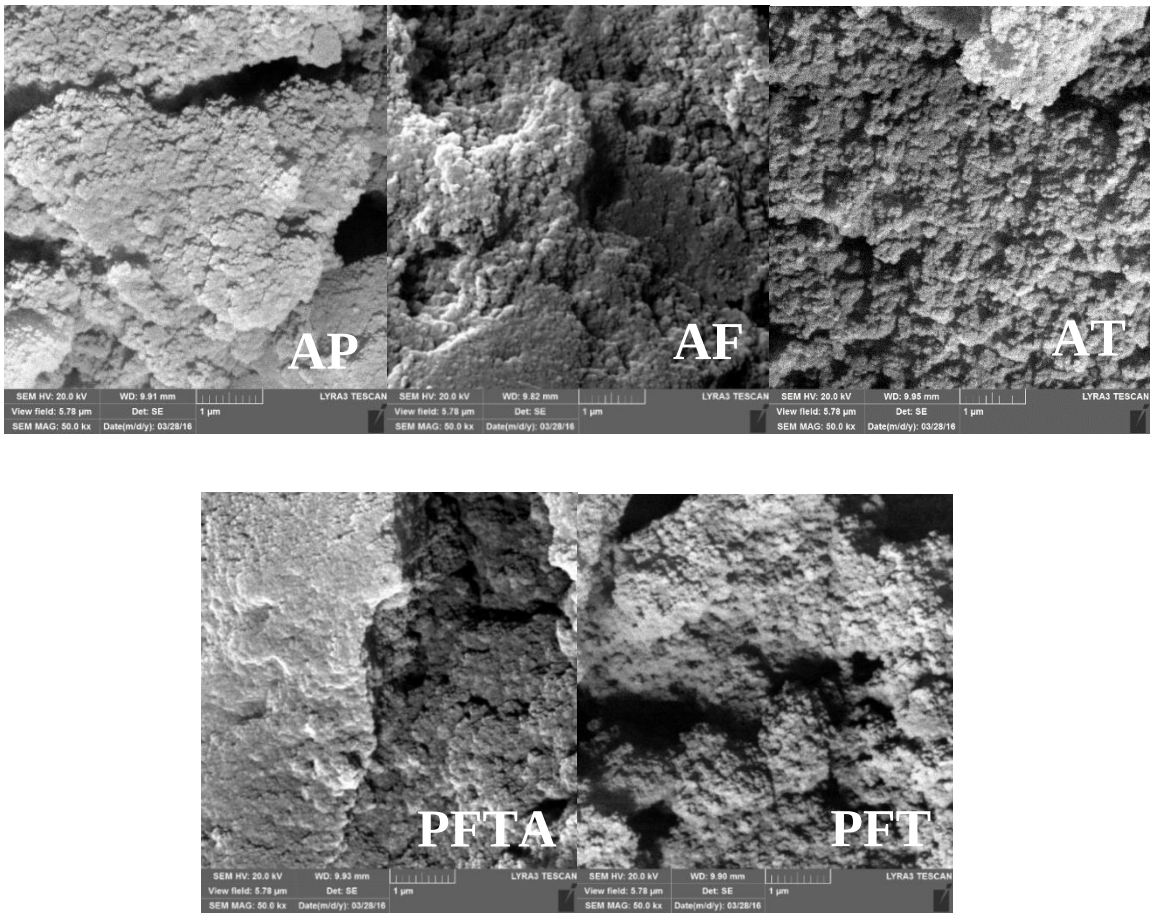

Figure 31 SEM images for all the polymers scaled up to 1 micrometer as indicated on each image

3.4 Gas Adsorption Calculations and Characterization

3.4.1 Isotherm characterization & Surface area

Nitrogen gas isotherms at 77K were measured for the polymers to calculate the surface area, pore volume and pore sizes, and all of the data are tabulated in (**Table 12**)

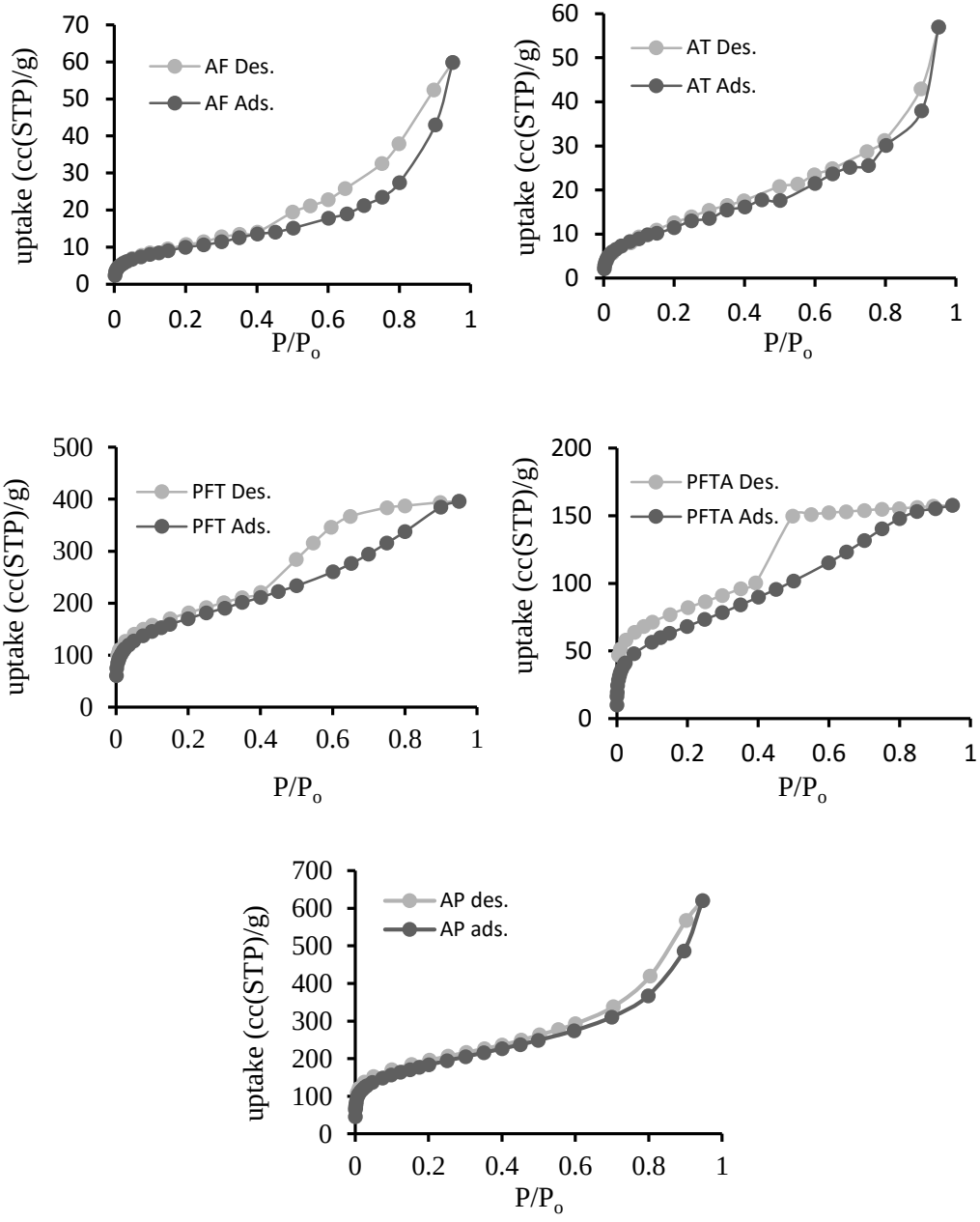

Figure 32 Gas adsorption isotherms for N_2 at 77K for all the polymers AP, AF, AT, PFT and PFTA

Nitrogen Isotherms given in (**Figure 32**) show different pore nature for different polymers. The Aniline-Furan (AF) and Aniline-Thiophene (AT) polymers had low total nitrogen uptake with very low uptake in the region of low relative pressure which means that they lack microporosity and the uptake is most likely because of the macropore nature that can be distinguished because of condensation behavior at high relative pressure, these isotherms can be assigned as type II isotherms. Also the hysteresis in the AF polymer is a H3 type that is assigned because of one of two reasons, the first is particles may form a non-rigid aggregates and causes this behavior or the second which proposes the presence of partially filled macropores in the network.

The PFT and PFTA polymers isotherms show relatively high uptake at very low relative pressure that corresponds to micropore nature of the material, and this can also be assured form the micropore calculations presented in (**Table 12**). The isotherms are not typical to be classified with certainty, though they have the hysteresis mode and behavior that resembles a type IV isotherm [25].

Table 12 Surface area of different polymers using BET and Langmuir models

Polymer name	BET (m^2/g)	Langmuir (m^2/g)	Micropore volume[(a)] (cc/g)	Pore radius[(a)] (Å)
AP	645	861	0.289	8.100
AF	36	52	0.012	8.900
AT	44	69	0.016	9.400
PFT	558	697	0.227	8300
PFTA	250	353	0.159	9.400

(a) Both micropore volume and pore radius were calculated using the Dubinin-Astakhov (DA) method.

3.4.2 Pore Size Distribution

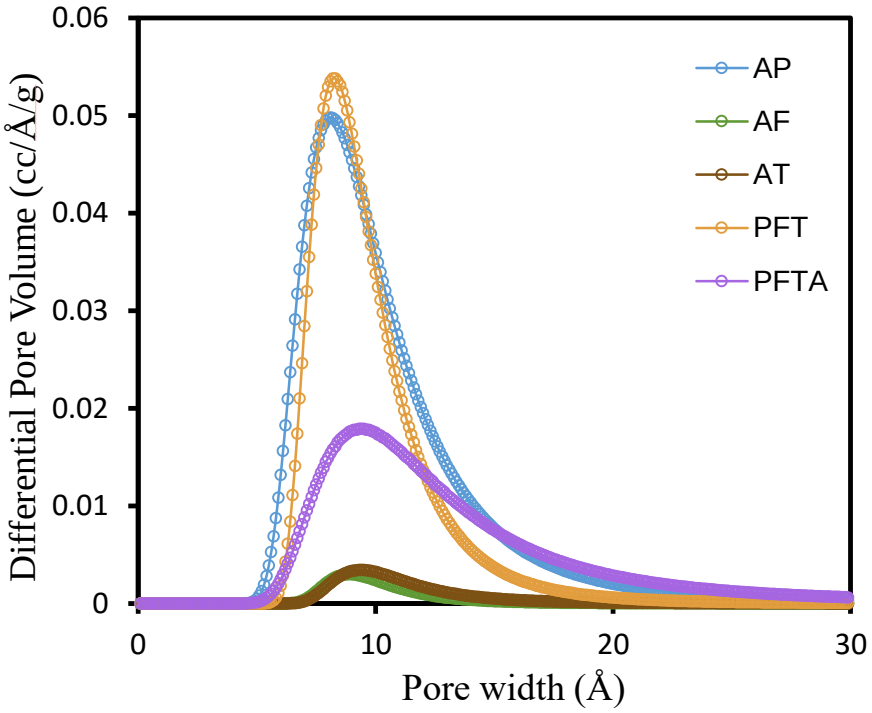

Figure 33 Pore size distribution in the micro region for the whole series as measured by Dubinin-Astrakhov (DA) method

The pore size distribution for the polymers in the micropore region show huge variety among the polymers with the AP and PFT have the highest curve area and hence, highest pore volume. AP and PFT also show relatively narrow distribution region concentrated around 10 Å. PFTA comes next in terms of pore volume and shows a kind of broader distribution compared to what found in AP and PFT. AT and AF came at the end with very low and very similar pore volume.

3.4.3 Gas uptake measurements

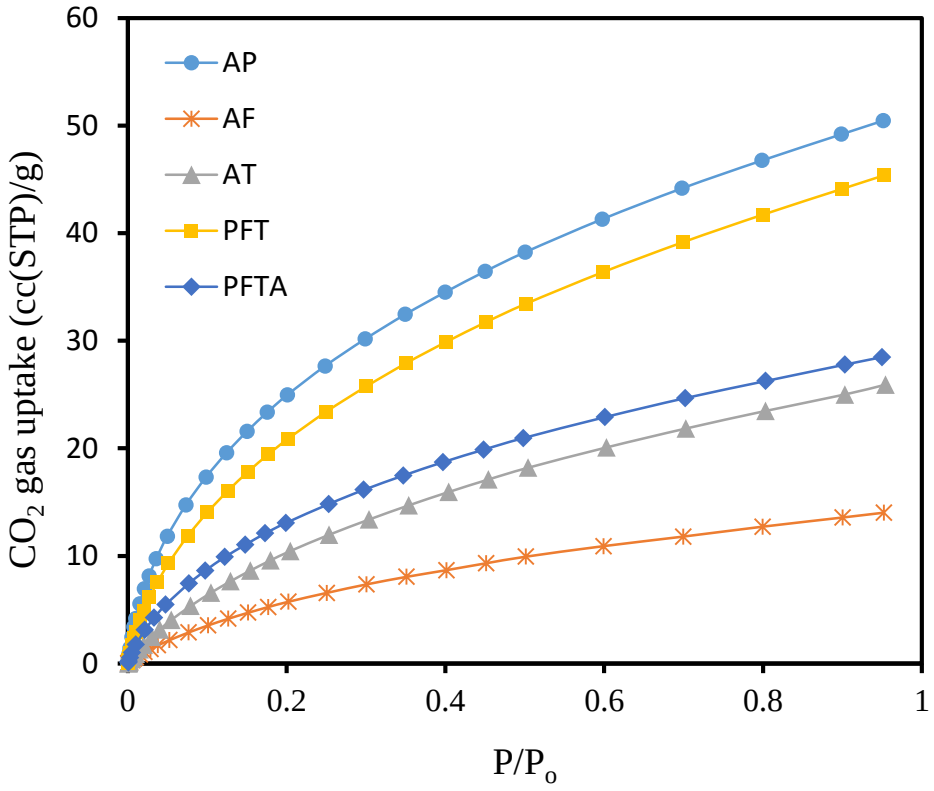

Figure 34 CO_2 Gas uptake comparison between all the polymers

The polymers were tested for the CO_2 adsorption at 273K in order to determine their capture property and which material to keep working on. Isotherms of the adsorption are provided in (**Figure 34**). The CO_2 uptake achieved at 273K is 14.1 cc/g and 25.9 cc/g for AF and AT respectively and it can be noticed that these results lag far behind what AP scored at same temperature and relative pressure. Then PFT and PFTA scored 45.4 cc/g and 28.5 cc/g respectively.

Since that among all the newly synthesized polymers only PFT showed a promising uptake capacity and relatively high surface area, PFT polymer was further investigated as will be discussed in (Section 3.5).

3.5 A detailed study on PFT adsorption properties

Depending on the data obtained from the pore size distribution, surface area and CO_2 uptake for the polymers, we found that AP and PFT polymers are the main polymers that worth a full gas sorption study. Since AP polymer was already studied in details in (Chapter 2), the focus will be only on the PFT polymer. The polymer was tested for CO_2 again but at three different temperatures 273K, 298K and 313K and then tested for its uptake capability for other gases, N_2 and CH_4, that have high contribution in the composition of flue gas in order to examine the material for real life application.

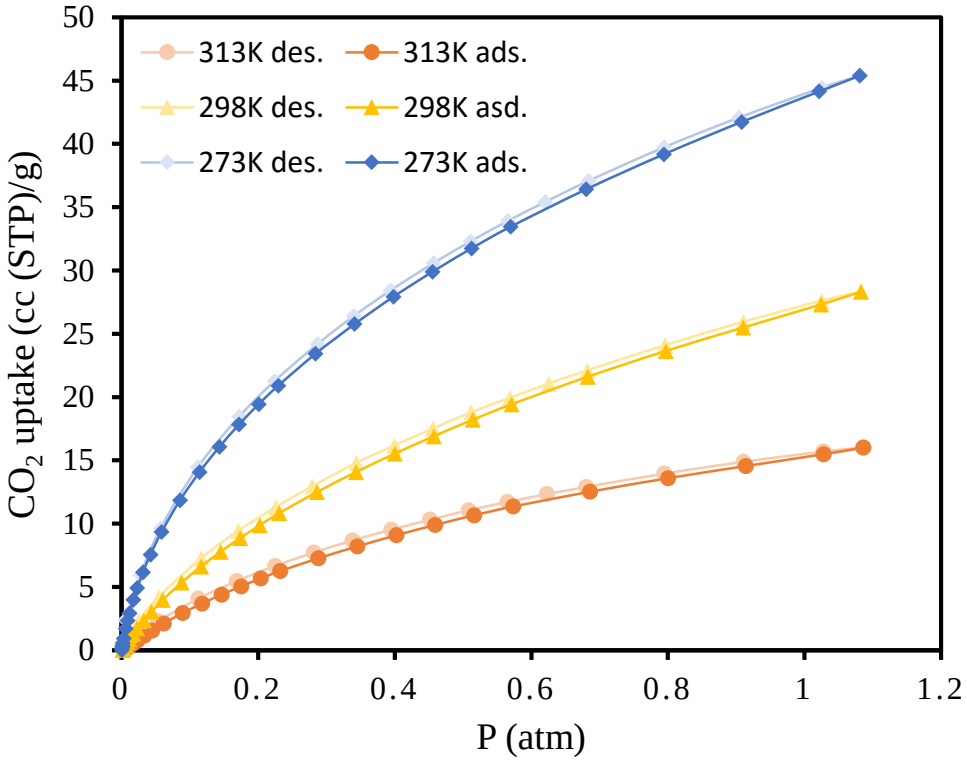

Figure 35 CO_2 gas uptake for PFT polymer at different temperatures 273K, 298K and 313K

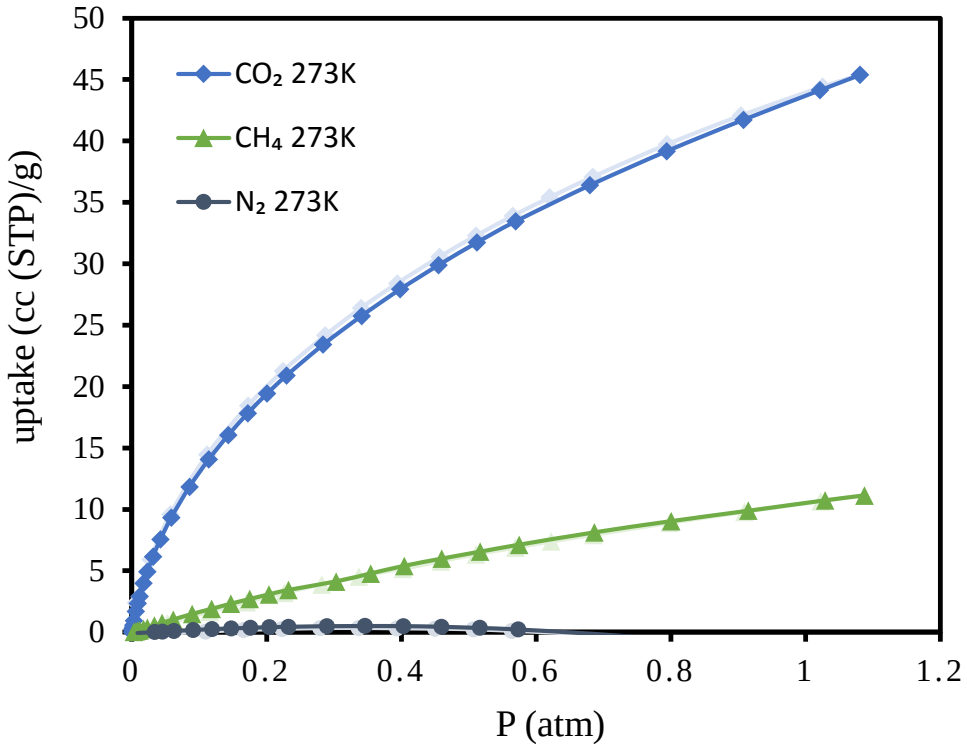

Figure 36 Different gas uptake of CO_2, CH_4 and N_2 for PFT polymer at same temperature (273K)

The isotherms in (**Figure 36**) were used to calculate the selectivity of the PFT polymer for CO_2 over CH_4 and N_2 gases.

3.5.1 Selectivity Measurements

As discussed in (Chapter 2) for AP polymer, the selectivity measurements were conducted for the PFT polymer in the same manner using the **Initial Slope Selectivity** and **Henry's Law Selectivity methods**

3.5.1.1 Initial Slope Selectivity

Data obtained from different gas isotherms at 273K were used to calculate the initial selectivity as indicated in (**Figure 37**).

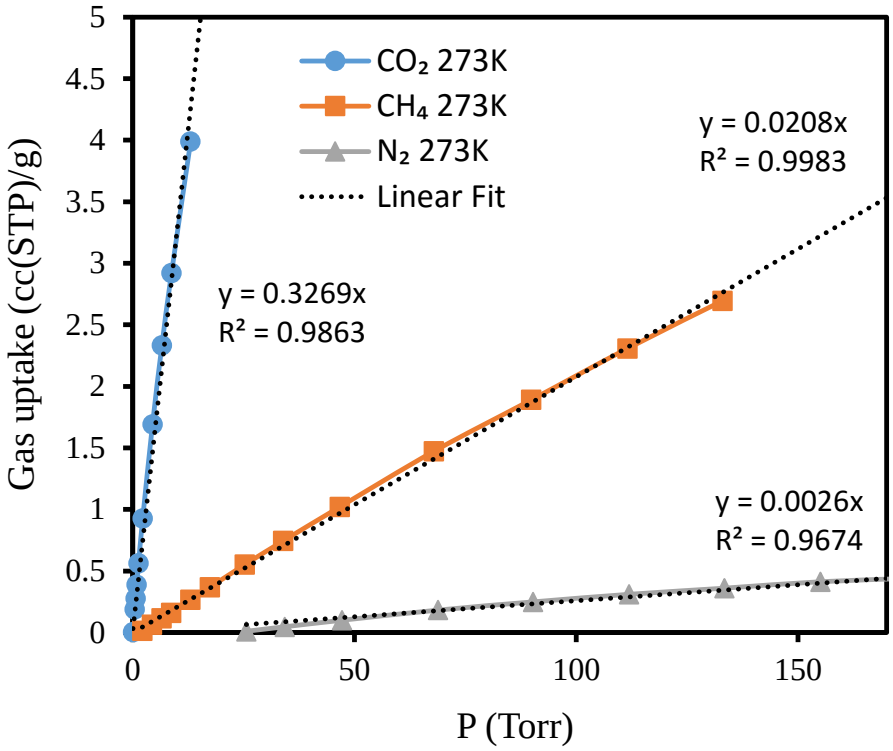

Figure 37 Initial slope selectivity curves and their linear fitting using the experimental data points

Table 13 Parameters for initial slope selectivity for CO_2, CH_4 and N_2

Gas type	Equation	CC (R^2)	Slope	Intercept
CO_2	$y= K_a*x$	0.9863	0.3269	0
CH_4	$y= K_b*x$	0.9983	0.0208	0
N_2	$y= K_c*x$	0.9674	0.0026	0

Selectivity CO_2/CH_4	16	Selectivity CO_2/N_2	126

3.5.1.2 Selectivity by Henry's Law

Dual-site Langmuir model fit was applied on the isotherms in order to get reasonable data. The fitting curves and the fitting parameters are provided in (Figure 38) and (**Table 14**) respectively.

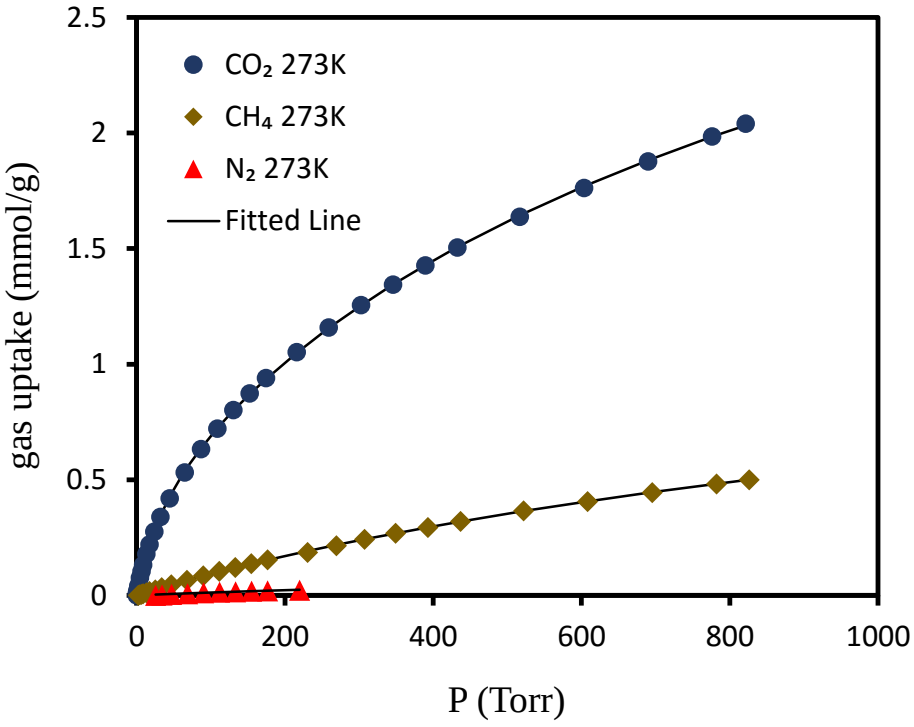

Figure 38 (PFT) polymer Experimental and Langmuir fitting calculated data of isotherms of CO_2, CH_4 and N_2 at 273K.

Table 14 Fitting parameters of dual-site Langmuir model for PFT polymer for CO_2, CH_4 and N_2 isotherms at 273K

Parameter	CO_2	CH_4	N_2
q_{m1}	0.54731	0.04303	0.06077
q_{m2}	3.43115	1.48703	0.09444
a_1	0.02480	0.00539	0.00082

a_2	0.00096	0.00055	0.00082
K_H	0.01686	0.00105	0.00013
error	0.00059	0.00008	0.00002

Selectivity CO_2/CH_4	16	Selectivity CO_2/N_2	133

3.5.2 Estimation of Isosteric heat of Adsorption (Q_{st})

A virial-type equation was used for the fitting of the experimental data, and Fitting curves of the isotherms and fitting parameters obtained from the iterations are given in (**Figure 39**) and (**Table 15**) respectively.

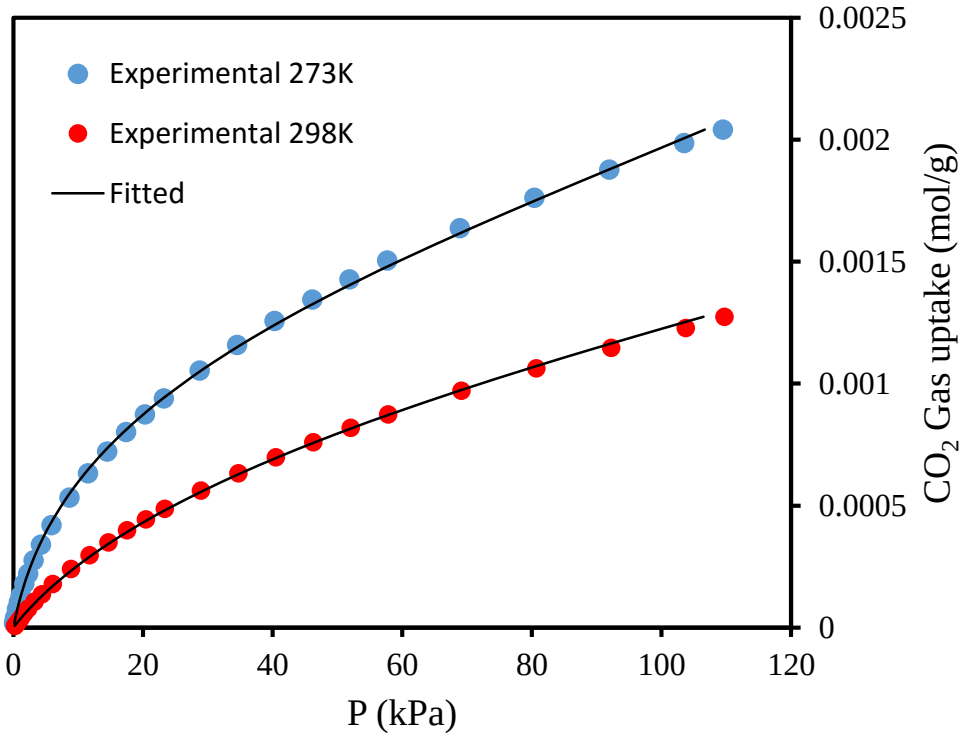

Figure 39 Fitting curves from the virial-type equation for CO_2 isotherms at 273K and 298K

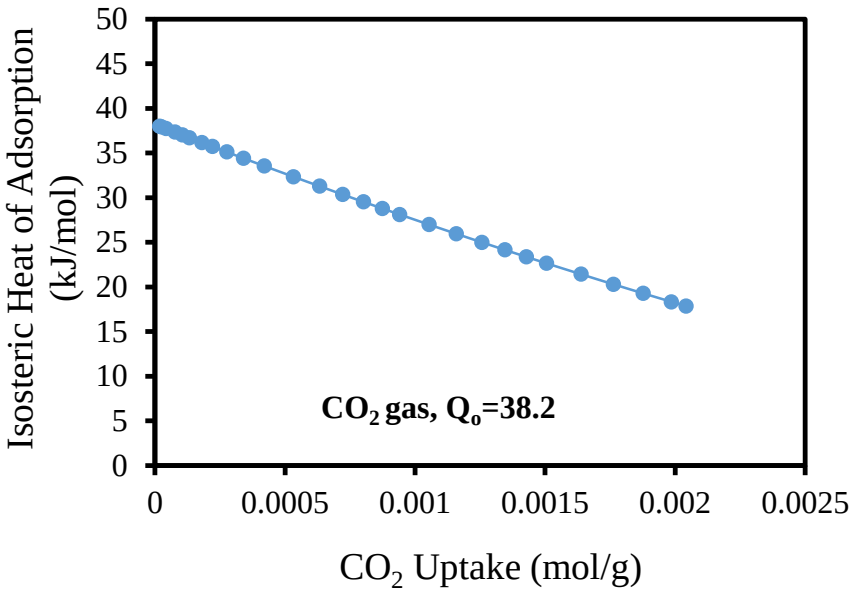

Figure 40 Isosteric heat of adsorption (Qst) curve as calculated from the virial coefficients

Table 15 Fitting parameters used in the virial-type equation fitting of CO_2 isotherms at 273K and 298K for PFT

Parameter	CO_2
a_0	-4594.895052
a_1	1367788.808
a_2	-82748014.51
b_0	32.6229783
b_1	-3421.646081
Error (σ^2)	0.0053
Q_0 (kJ/mol)	38.2

3.6 Literature Comparison

In order to give sense to the results, and to estimate how efficient the synthesized polymers are, a comparison was made between the best polymers in this study which are AP and PFT polymers and other materials from literature that may or may not be classified as similar materials but were used for the same application.

Table 16 Comparison table between the results of this work with other works in literature

Polymeric material	CO_2 uptake[1] (mmol/g)	Selectivity[2]		SA/BET (m^2/g)	Q_{st}	reference
		CO_2/N_2	CO_2/CH_4			
DMAc-NMP	0.134	-	-	84.5	-	[43]
Py-1, Fu-1 & Th-1	2.06 - 2.88	39 - 117	-	437-726	27 - 36	[15]
BILPs	5.5	113	17	599-1306	~28	[44]
COFs	1.3 - 3.8	-	-	750- 3500	-	[45]
PPNs	4.2	-	-	6461	-	[46]
STB-60DVB-d	1.29 273K 1.03 298K	-	-	559	-	[47]
CMPs	1.18 298K	-	-	837	27	[48]
Co-polymer network	1.18 300K	16 - 49	-	10 - 1289	-	[35]
AP	**2.3 273K 1.5 298K**	**89**	**18**	**645**	**~37**	**This work**
PFT	**2.0 273K 1.3 298K**	**133**	**16**	**588**	**~38**	**This work**

[1] All provided uptakes were measured at 273K and 1 atm unless other conditions are written.
[2] Selectivity was measured from isotherms at 273K using Henry's Law.

References

[1] S. A. Didas, S. Choi, W. Chaikittisilp, and C. W. Jones, "Amine-Oxide Hybrid Materials for CO_2 Capture from Ambient Air," *Acc. Chem. Res.*, vol. 48, no. 10, pp. 2680–2687, 2015.

[2] E. J. García, J. Pérez-Pellitero, G. D. Pirngruber, C. Jallut, M. Palomino, F. Rey, and S. Valencia, "Tuning the adsorption properties of zeolites as adsorbents for CO_2 separation: Best compromise between the working capacity and selectivity," *Ind. Eng. Chem. Res.*, vol. 53, no. 23, pp. 9860–9874, 2014.

[3] P. Puthiaraj and W. Ahn, "CO_2 Capture by Porous Hyper-Cross-Linked Aromatic Polymers Synthesized Using Tetrahedral Precursors," 2015.

[4] H. Furukawa, K. E. Cordova, M. O'Keeffe, and O. M. Yaghi, "The chemistry and applications of metal-organic frameworks.," *Science*, vol. 341, no. 6149, p. 1230444, Aug. 2013.

[5] S. Cui, W. Cheng, X. Shen, M. Fan, A. (Ted) Russell, Z. Wu, and X. Yi, "Mesoporous amine-modified SiO_2 aerogel: a potential CO_2 sorbent," *Energy Environ. Sci.*, vol. 4, no. 6, p. 2070, 2011.

[6] Y. Shi, J. Zhu, X. Liu, J. Geng, and L. Sun, "Molecular Template-Directed Synthesis of Microporous Polymer Networks for Highly Selective CO_2 Capture.," *ACS Appl. Mater. Interfaces*, vol. 6, no. 22, pp. 20340–9, 2014.

[7] P. Arab, A. Verlander, and H. M. El-Kaderi, "Synthesis of a highly porous bis(imino)pyridine-linked polymer and its postsynthetic modification with inorganic fluorinated ions for selective CO_2 capture," *J. Phys. Chem. C*, vol. 119, no. 15, pp. 8174–8182, 2015.

[8] D. Lee, C. Zhang, and H. Gao, "Amine-Functionalized Porous Polymer Network for Highly Selective Absorption of CO_2 Over N_2," *Macromol. Chem. Phys.*, vol. 216, no. 5, pp. 489–494, 2015.

[9] H. a. Patel, S. H. Je, J. Park, D. P. Chen, Y. Jung, C. T. Yavuz, and A. Coskun, "Unprecedented high-temperature CO_2 selectivity in N2-phobic nanoporous covalent organic polymers.," *Nat. Commun.*, vol. 4, p. 1357, 2013.

[10] A. Torrisi, R. G. Bell, and C. Mellot-Draznieks, "Functionalized MOFs for enhanced CO_2 capture," *Cryst. Growth Des.*, vol. 10, no. 7, pp. 2839–2841, 2010.

[11] D. Aaron and C. Tsouris, "Separation of CO2 from Flue Gas: A Review," *Sep. Sci. Technol.*, vol. 40, no. 1, pp. 321–348, 2005.

[12] K. Sumida, D. L. Rogow, J. a Mason, T. M. Mcdonald, E. D. Bloch, Z. R. Herm, T. Bae, and J. R. Long, "Carbon Dioxide Capture in Metal- Organic Frameworks," *Chem. Rev.*, vol. 112, pp. 724–781, 2012.

[13] D. Li, H. Furukawa, H. Deng, C. Liu, O. M. Yaghi, and D. S. Eisenberg,

"Designed amyloid fibers as materials for selective carbon dioxide capture.," *Proc. Natl. Acad. Sci. U. S. A.*, vol. 111, no. 1, pp. 191–6, 2014.

[14] P. A. Kumar, M. Ray, and S. Chakraborty, "Hexavalent chromium removal from wastewater using aniline formaldehyde condensate coated silica gel," *J. Hazard. Mater.*, vol. 143, no. 1–2, pp. 24–32, 2007.

[15] Y. Luo, B. Li, W. Wang, K. Wu, and B. Tan, "Hypercrosslinked aromatic heterocyclic microporous polymers: A new class of highly selective CO_2 capturing materials," *Adv. Mater.*, vol. 24, no. 42, pp. 5703–5707, 2012.

[16] M. A. Quraishi and S. K. Shukla, "Poly(aniline-formaldehyde): A new and effective corrosion inhibitor for mild steel in hydrochloric acid," *Mater. Chem. Phys.*, vol. 113, no. 2–3, pp. 685–689, 2009.

[17] R. R. Koner, P. A. Kumar, S. Chakraborty, and M. Ray, "Synthesis of Morphologically Different, Metal Absorbing Aniline-Formaldehyde Polymers Including Micron-Sized Sphere Using Simple Alcohols as Morphology Modifier," *Appl. Polym. Sci.*, vol. 110, pp. 1158–1164, 2008.

[18] Y. Zhang, M. Nie, X. Wang, Y. Zhu, F. Shi, J. Yu, and B. Hou, "Effect of molecular structure of aniline-formaldehyde copolymers on corrosion inhibition of mild steel in hydrochloric acid solution," *J. Hazard. Mater.*, vol. 289, pp. 130–139, 2015.

[19] G. Liu and M. S. Freund, "New Approach for the Controlled Cross-Linking of Polyaniline : Synthesis and Characterization," *Macromolecules*, vol. 9297, no. 97, pp. 5660–5665, 1997.

[20] H. Tang, J. Wang, H. Yin, H. Zhao, D. Wang, and Z. Tang, "Growth of polypyrrole ultrathin films on mos2 monolayers as high-performance supercapacitor electrodes," *Adv. Mater.*, vol. 27, no. 6, pp. 1117–1123, 2015.

[21] T. Yamamoto, Y. Yamagata, R. Yamashita, M. Abla, H. Fukumoto, and T. A. Koizumi, "Copolymers of pyrrole with N-alkynylpyrroles," *Synth. Met.*, vol. 162, no. 24, pp. 2406–2413, 2012.

[22] Z. Xiang, R. Mercado, J. M. Huck, H. Wang, Z. Guo, W. Wang, D. Cao, M. Haranczyk, and B. Smit, "Systematic Tuning and Multifunctionalization of Covalent Organic Polymers for Enhanced Carbon Capture," *J. Am. Chem. Soc.*, vol. 137, no. 41, pp. 13301–13307, 2015.

[23] S. Yao, X. Yang, M. Yu, Y. Zhang, and J.-X. Jiang, "High surface area hypercrosslinked microporous organic polymer networks based on tetraphenylethylene for CO2 capture," *J. Mater. Chem. A*, vol. 2, pp. 8054–8059, 2014.

[24] G. Liu, Y. Wang, C. Shen, and D. Yuan, "A facile synthesis of microporous organic polymers for efficient gas storage and separation," *J. Mater. Chem. A*, vol. 3, pp. 3051–3058, 2015.

[25] M. Thommes, K. Kaneko, A. V. Neimark, J. P. Olivier, F. Rodriguez-Reinoso, J.

Rouquerol, and K. S. W. Sing, “Physisorption of gases, with special reference to the evaluation of surface area and pore size distribution (IUPAC Technical Report),” *Pure Appl. Chem.*, vol. 87, no. 9–10, pp. 1051–1069, 2015.

[26] X. Wang, Y. Zhao, L. Wei, C. Zhang, and J.-X. Jiang, “Nitrogen-rich conjugated microporous polymers: impact of building blocks on porosity and gas adsorption,” *J. Mater. Chem. A*, vol. 3, pp. 21185–21193, 2015.

[27] S. Wu, Y. Liu, G. Yu, J. Guan, C. Pan, Y. Du, X. Xiong, and Z. Wang, “Facile preparation of dibenzoheterocycle-functional nanoporous polymeric networks with high gas uptake capacities7,” *Macromolecules*, vol. 47, no. 9, pp. 2875–2882, 2014.

[28] Quantachrome Instruments, *auto sorb iQ and ASiQwin GAS SORPTION SYSTEM*. 2013.

[29] B. Nie, X. Liu, L. Yang, J. Meng, and X. Li, “Pore structure characterization of different rank coals using gas adsorption and scanning electron microscopy,” *Fuel*, vol. 158, pp. 908–917, 2015.

[30] S.-C. Xiang, Z. Zhang, C.-G. Zhao, K. Hong, X. Zhao, D.-R. Ding, M.-H. Xie, C.-D. Wu, M. C. Das, R. Gill, K. M. Thomas, and B. Chen, “Rationally tuned micropores within enantiopure metal-organic frameworks for highly selective separation of acetylene and ethylene.,” *Nat. Commun.*, vol. 2, p. 204, 2011.

[31] W. L. Queen, E. D. Bloch, C. M. Brown, M. R. Hudson, J. A. Mason, L. J. Murray, A. J. Ramirez-Cuesta, V. K. Peterson, and J. R. Long, “Hydrogen adsorption in the metal–organic frameworks Fe_2(dobdc) and Fe2(O_2)(dobdc),” *Dalt. Trans.*, vol. 41, no. 14, p. 4180, 2012.

[32] L. Czepirski and J. Jagiello, “Virial-type thermal equation of gas-solid adsorption,” *Chem. Eng. Sci.*, vol. 44, no. 4, pp. 797–801, 1989.

[33] C. W. Bird, “HETEROAROMATICITY , S . A UNIFIED AROMATICITY INDEX,” *Tetrahedron*, vol. 48, no. 2, pp. 335–340, 1992.

[34] C. P. Frizzo and M. A. P. Martins, “Aromaticity in heterocycles : new HOMA index parametrization,” *Struct. Chem.*, vol. 23, pp. 375–380, 2012.

[35] R. Dawson, T. Ratvijitvech, M. Corker, A. Laybourn, Y. Z. Khimyak, A. I. Cooper, and D. J. Adams, “Microporous copolymers for increased gas selectivity,” *Polym. Chem.*, vol. 3, no. 8, p. 2034, 2012.

[36] T. Narasimhaswamy, D. K. Lee, K. Yamamoto, N. Somanathan, and A. Ramamoorthy, “A 2D solid-state NMR experiment to resolve overlapping aromatic resonances of thiophene-based nematogens,” *J. Am. Chem. Soc.*, vol. 127, no. 19, pp. 6958–6959, 2005.

[37] Q. Tian, Y. C. Yuan, M. Z. Rong, and M. Q. Zhang, “A thermally remendable epoxy resin,” *J. Mater. Chem.*, vol. 19, no. 9, p. 1289, 2009.

[38] Z. Wu, C. Li, Z. Wei, P. Ying, and Q. Xin, “FT-IR Spectroscopic Studies of

Thiophene Adsorption and Reactions on Mo_2N / γ-Al2O3 Catalysts," *J. Phys. Chem. B*, vol. 106, pp. 979–987, 2002.

[39] M. González-torres, M. G. Olayo, G. J. Cruz, L. M. Gómez, V. Sánchez-mendieta, and F. González-salgado, "XPS Study of the Chemical Structure of Plasma Biocopolymers of Pyrrole and Ethylene Glycol," *Adv. Chem.*, vol. 2014, pp. 1–8, 2014.

[40] C. Zhang, W. Song, G. Sun, L. Xie, J. Wang, K. Li, C. Sun, H. Liu, C. E. Snape, and T. Drage, "CO2 capture with activated carbon grafted by nitrogenous functional groups," *Energy and Fuels*, vol. 27, no. 8, pp. 4818–4823, 2013.

[41] E. Melnik, P. Muellner, O. Bethge, E. Bertagnolli, R. Hainberger, and M. Laemmerhofer, "Streptavidin binding as a model to characterize thiol-ene chemistry-based polyamine surfaces for reversible photonic protein biosensing," *Chem. Commun.*, vol. 50, no. 19, pp. 2424–2427, 2014.

[42] J. W. F. To, J. He, J. Mei, R. Haghpanah, Z. Chen, T. Kurosawa, S. Chen, W.-G. Bae, L. Pan, J. B.-H. Tok, J. Wilcox, and Z. Bao, "Hierarchical N-Doped Carbon as CO2 Adsorbent with High CO2 Selectivity from Rationally Designed Polypyrrole Precursor," *J. Am. Chem. Soc.*, vol. 138, pp. 1001 – 1009, 2016.

[43] S. Zulfiqar, M. I. Sarwar, and C. T. Yavuz, "Melamine based porous organic amide polymers for CO2 capture," *RSC Adv.*, vol. 4, no. 94, pp. 52263–52269, 2014.

[44] M. G. Rabbani and H. M. El-kaderi, "Synthesis and Characterization of Porous Benzimidazole-Linked Polymers and Their Performance in Small Gas Storage and Selective Uptake," *Chem. Mater.*, vol. 24, pp. 1511–1517, 2012.

[45] H. Furukawa and O. M. Yaghi, "Storage of Hydrogen, Methane, and Carbon Dioxide in Highly Porous Covalent Organic Frameworks for Clean Energy Applications," *J. Am. Chem. Soc.*, vol. 131, no. 25, pp. 8875–8883, 2009.

[46] D. Yuan, W. Lu, D. Zhao, and H. C. Zhou, "Highly stable porous polymer networks with exceptionally high gas-uptake capacities," *Adv. Mater.*, vol. 23, no. 32, pp. 3723–3725, 2011.

[47] J. Huang, X. Zhou, A. Lamprou, F. Maya, F. Svec, and S. R. Turner, "Nanoporous Polymers from Cross-Linked Polymer Precursors via tert-Butyl Group Deprotection and Their Carbon Dioxide Capture Properties," *Chem. Mater.*, vol. 27, no. 21, pp. 7388–7394, 2015.

[48] R. Dawson, D. J. Adams, and A. I. Cooper, "Chemical tuning of CO_2 sorption in robust nanoporous organic polymers," *Chem. Sci.*, vol. 2, no. 6, p. 1173, 2011.

Vitae

Name	: Ahmed Mohamed Alloush
Nationality	: Egyptian
Date of Birth	: 02/02/1991
Email	: ahmad.m.alloush@gmail.com
Address	: Al-Askaryah street, Damanhur, Beheira, Egypt
Academic Background	: Chemistry